DOI: xx.xxxx/ ((please add manuscript number))

Article type: Review

Near-infrared (NIR) Organic light-emitting diodes (OLEDs): challenges and opportunities

*Andrea Zampetti, Alessandro Minotto, and Franco Cacialli**

Dr. A. Zampetti, Dr. A. Minotto, Prof. F. Cacialli,

Department Physics and Astronomy and London Centre for Nanotechnology

University College London,

London, WC1H 0AH, United Kingdom

E-mail: f.cacialli@ucl.ac.uk

Keywords: OLED, near-infrared, blend

Biography:

Andrea Zampetti obtained his MSc and Ph.D. in Telecommunication and Microelectronic Engineering from the University of Rome "Tor Vergata" (Italy), in 2011 and 2015, respectively. He was awarded a Marie Curie Early Stage Researcher Fellowship under the FP7 ITN OSNIRO project (Organic Semiconductors for NIR optoelectronics) at the London Centre for Nanotechnology in 2014. During this period, he worked on the characterization and fabrication of NIR OLEDs based on purely organic emitters. He is currently the Scientific Project Manager of a European H2020 MSCA ITN project at UCL.

Alessandro Minotto received his MSc and PhD in Materials Science from the University of Padova, in 2011 and 2015, respectively. After this, he was appointed as Marie Curie Early Stage Researcher Fellow under the FP7 ITN project on Organic Semiconductors for NIR Optoelectronics (OSNIRO) in the London Centre for Nanotechnology. He is now a research fellow in the Department of Physics and Astronomy at UCL, funded by the EPSRC project on Multifunctional Polymer Light-Emitting Diodes with Visible Light Communications (MARVEL).

Franco Cacialli received his Ph.D. degree in Electronic Engineering from the University of Pisa in 1994. Since 2005, he has been Professor of Physics in the London Centre for Nanotechnology (London Centre for Nanotechnology (LCN, http://www.london-nano.com/) and the Department of Physics and Astronomy at University College London. After postdoctoral work at Cambridge, he was a Royal Society University Research Fellow (1996–2004), first at Cambridge (until 2001), then at UCL. He has coordinated a Marie Curie Research Training Network dedicated to investigation of threaded molecular wires (www.threadmill.eu) and currently coordinates a European Training Network dedicated to exploitation of supramolecular materials for photonics (synchronics-etn.eu). A Fellow of the Institute of Physics (FinstP, 2001), and of the American Physical Society (2009), he currently is a recipient of a Royal Society Wolfson Research Merit Award (2015–2019) and a co-director of the recently formed London Institute for Advanced Light Technologies (london-light.org).

The rapid development of the science and technology of organic semiconductors has already led to mass application of organic light-emitting diodes (OLEDs) in TV monitors of outstanding quality as well as in a large variety of smaller displays found in smartphones, tablets and other gadgets, while introduction of the technology to the illumination sector is imminent. Notably, the requirements of all such applications for emission in the visible range of the electromagnetic spectrum are well tuned to the optical and electronic properties of typical organic semiconductors, thereby representing relatively "low-hanging fruits", in terms of materials development and exploitation. However, the question arises as to whether developing materials suited for efficient near-infrared (NIR, 700-1000 nm) emission is possible, and, crucially, desirable to enable new classes of applications spanning from through-space, short-range communications, to biomedical sensors, night vision and more generally security applications to name but a few. In the following we discuss the major fundamental hurdles to be overcome to achieve efficient NIR emission from organic π-conjugated systems, we review recent progress, and provide an outlook for further development of both materials and applications.

1. Introduction

Organic light-emitting diodes (OLEDs) are devices based on a deceptively simple sandwich structure in which an organic semiconductor material is sandwiched between two electrodes for injection of oppositely-signed carriers (electrons and holes). The active material, which can also be a blend, acts as both a chromophore and a charge transport medium. Electrons and holes injected from the electrodes drift and diffuse within the active layer under the action of the applied potential and concentration gradients, and mutually capture with good efficiency thanks to poorly-screened coulombic interactions, thereby forming bound electron-hole pairs, or excitons, which are then susceptible of radiative decay. Despite such a simple structure and operation mechanism, a few decades have proved necessary to bring the initial discoveries[1] to commercial fruition via materials and device engineering, that have progressively enhanced device parameters such as efficiency, luminance, operating voltages, and most importantly durability, until suitable for commercialisation. Among others, important advances included development of chromophores with progressively higher efficiency in the solid state, e.g. via control of aggregation,[2] or via harvesting of both singlet and triplet excitons,[3] of charge transport groups/materials to be blended or covalently linked to the chromophores, or added as additional interlayers between electrodes and active layers, as well as optimisation of the energy level alignment at the interfaces, so as to optimise charge injection.[4]

The fortunate coincidence that π-conjugated systems have energy structures suited for emission in the visible range of the electromagnetic spectrum, together with the ease of tailoring of the chemical (and electronic) structure of the materials afforded by organic chemistry have allowed development of "libraries of materials" covering the whole gamut of visible colours, with a few examples even extending in the (near) UV range (below 400 nm)[5] and, increasingly so, in the near-infrared (NIR).[6] We show in **Figure 1** the evolution of the number of relevant publications (search criteria "Near-infrared" and "Emission" and "Organic") as found in the

Web of Knowledge database in September 2018 (the apparent decline for the last year is only due to the search being conducted during the year, and not accounting for it "pro rata").

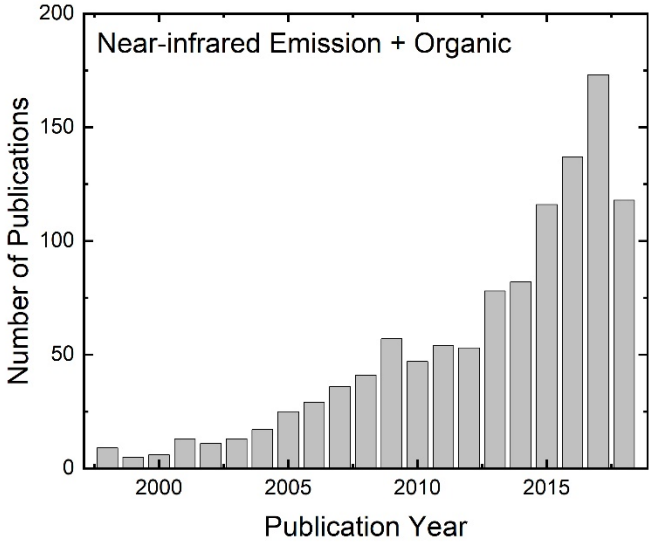

Figure 1. Number of publications on organic near-infrared emission published over the past twenty years as counted by the Institute for Scientific Information (ISI) Web of Science, as of 18th September 2018. The search criteria are "Near-infrared" and "Emission" and "Organic".

It is important to note here that there is actually little consensus in the literature on the definition of the longer-wavelength end of the NIR range, whereas the shorter wavelength end is usually taken to be 700 nm. In the following we will focus our attention mostly on the range extending from such a wavelength (700 nm, or ~ 1.77 eV, i.e. the "high-energy" limit) and 1000 nm (~ 1.24 eV, or the "low-energy limit") and refer to this range as the NIR, even though we are aware some texts extend the definition of this range up to 2 or even 3 μm on the low-energy side.

The reason for our choice is twofold: first of all the 700-1000 nm window coincides with the biological tissue semitransparency window (see **Figure 2** below)[7] which makes it interesting for application of NIR-OLEDs to a variety of biomedical and biosensing applications. Secondly, emission in the solid state at wavelengths beyond 1000 nm is rather

weak for organic chromophores thereby calling into question their use, even in the presence of other advantages such as flexibility, low-cost, potential biocompatibility etc.

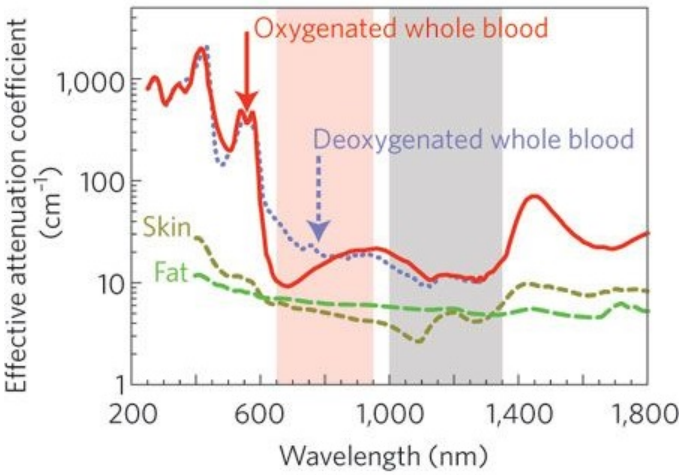

Figure 2. Biological tissue semitransparency window.[7]
Adapted with permission.[7] Copyright 2009, SMITH/MANCINI/NIE.

Interestingly, pursuit of NIR emission instead of UV comes in principle with an inherent bonus in terms of materials stability and thus devices durability. The energy involved with generation and decay of the excited species (charged and neutral) is in fact much smaller for NIR than for UV emission (~1.1-1.8 eV in the 700-1000 nm window vs. ≥ 3.1 eV for emission below 400 nm), thereby limiting the scope for side-reactions to take place, and increasing the expected stability of materials and devices. Indeed, the energies involved in UV electroluminescence (EL) processes, both the energy to generate the excitons and the energy released by the exciton upon non-radiative (mostly) and radiative decay, are relatively close to (or exceeding in some cases) those of the bonds.

Low-gap organic materials suitable for NIR emission also suffer, however, from significant lower luminescence efficiency when compared to visible emitters. This is generally understood to result from a combination of a greater tendency to form (detrimental) cofacial

(H) aggregates,[8] because of the need for more extended (planar) π systems to reduce the energy gap, and because of the so-called "Energy-gap" law,[9] which predicts a progressively greater likelihood of non-radiative deactivation of the excited states as the energy gap is reduced.

In the following we discuss first the opportunities offered and challenges posed by the potential development of NIR organic materials and devices (Section 2), we recall the main parameters that control the efficiency of OLEDs (Section 3), and then review current progress by looking first at materials and devices leveraging triplet emission, i.e. phosphorescent materials (Section 4), materials leveraging so-called thermally-activated delayed fluorescence, TADF (Section 5), and materials that only leverage singlet emission, or fluorescent materials (Section 6), which albeit less efficient than those relying on triplets harvesting offer the possibility of avoiding heavy metals (needed to enhance spin-orbit coupling and thus enable high luminescence efficiency in the case of the phosphorescent OLEDs), useful for biomedical in-vivo applications where toxicity is a concern, or to be driven at higher switching speeds, as required for example for through-space communications (e.g. in "visible" light communications (VLC)).[10]

Despite such hurdles, efficiencies up to 24 % (peaked at 740 nm) and emission peaked at 1 μm with a tail until 1.2 μm (with efficiency of ~ 0.3 %), respectively, have already been achieved by adopting careful design strategies of materials and devices.[6b, 11] The remarkable progress achieved by NIR OLEDs in the past few years guides further design and optimization of NIR emitters and provides a promising and encouraging outlook for development of this branch of organic electronics.

2. Opportunities and challenges

2.1 Application areas of NIR emitting (and absorbing materials)

Organic semiconductors with a narrow energy-gap are attractive for many applications leveraging NIR absorption, NIR emission, or both. Exploitation of NIR absorption for example is one of the main strategies to increase the power conversion efficiency (PCE) of organic (and inorganic) solar cells,[12] although it requires adoption of a tandem architecture so as to avoid degrading the open circuit voltage, and the PCE with it. A landmark result for organic photovoltaics has been obtained very recently with the attainment of PCEs over 17 %, thanks also to one of the materials used featuring an absorption edge near 1000 nm.[13] In addition, absorption in the NIR is also crucial for fabrication of NIR photodectors, with application to a number of imaging and (bio)sensing applications. Indeed, blood-oxymetry,[14] for example, ideally requires both absorption and emission in the NIR. The semi-transparency of biological tissue in the window 700-1000 nm makes this range particularly appealing for optical probes of analytes with absorption (and/or luminescence) in this range, as well as for photothermal and photodynamic therapeutic applications which may rely on photo-activation of particular drugs (e.g. to open cages containing suitable drugs in place of "redox-driven" breaking mechanisms),[15] or for therapy of sensitive tumours,[16] or even atherosclerosis treatment.[17]

NIR LEDs are often used also in security authentication technologies exploiting biometrics, such as imaging of finger veins[18] and iris recognition.[19]

Near-infrared LEDs could be also integrated as transmitters in Visible Light Communication (VLC) networks,[10] thereby offering the twofold benefit of extending the available bandwidth and being essentially invisible to the human eye.

Compared to quantum dots or perovskite LEDs, that can also be engineered for NIR emission, organic emitters do not require heavy metals mostly (with the exception of small

amounts in phosphorescent OLEDs) thereby becoming the elective choice for biomedical in-vivo applications where low-toxicity is of the essence.

Additional significant advantages of NIR-OLEDs compared to inorganic NIR emitters are afforded by their inherent flexibility and suitability for large area applications that, combined, afford unparalleled design freedom. This is appealing for example in developing new concepts, shapes and designs in "illumination" systems compared to inorganic emitters,[20] in particular by allowing a substantial substrates diversity (spanning from glasses, to ceramics, metals, thin plastic sheets, fabrics, flexible and more generally conformable substrates).[21] While it could be argued that illumination systems do not require NIR, by definition, we note that horticulture, for example does require some NIR illumination for the crops life-cycle management, and that NIR may usefully supplement the bandwidth of visible emitters in visible light communications (VLC) meant to be integrated with lighting systems. Distributing the emitter elements over large areas also allows driving the devices at lower intensities, therefore improving the heat dissipation requirements and facilitating integration in flexible systems.[22].

2.2 Device exploitation opportunities

Low-gap organic semiconductors (OS) also benefit from lower energetic barriers for injection of electrons compared to materials with a wider gap, thereby facilitating fabrication of devices exhibiting ambipolar charge-transport characteristics.[23] The reason for this is that for a large variety of OS, including narrow gap ones, the highest occupied molecular orbital (HOMO) occurs in a range approximately 4.7 – 6 eV below the vacuum level, thus enabling efficient hole-injection from materials conventionally employed as positive electrodes such as gold or indium tin oxide (ITO), that are characterised by work functions of ~ 5 eV or higher.[24] As a consequence, the lowest unoccupied molecular orbital, (LUMO) that must be offset with respect to the HOMO by the value of the energy gap, often ends up lying above 3 eV below the

vacuum level (i.e. electron affinities ~ 3 eV or less) for visible emitters. On the contrary, in narrow-gap OS, electron-injection is facilitated by deeper-lying LUMO levels (even below 4 eV below vacuum in some cases) therefore making it easier to obtain ambipolar transport characteristics from devices with symmetric electrodes.

Furthermore, and most relevant for OLEDs, the attainment of low energetic barriers between the electrodes and the active layer is desirable also because it eliminates the necessity of depositing additional interlayers to facilitate charge-injection, and therefore reduces the complexity (and the cost) of the final device.

2.3 Challenges

2.3.1 Reducing the gap

Traditionally, the opening of the energy gap in conjugated materials has been treated as originating from the bond-length difference between the alternating single and double bonds (Peierls dimerization). Such a gap is narrower in conjugated systems in which such a bond-length alternation (BLA) is reduced, thereby presenting an extended electron delocalization.[25]

In a prototypical polyenic, or polyyinic chain, the BLA can be engineered by structural modification of the conjugated backbone. However, the vast majority of commonly used OS contain aromatic rings, which add two further contributions to the overall energy-gap.[25b] The first one is the rotational disorder of aromatic rings around the main molecular axis, which limits the π-electron delocalization along the chain, and therefore raises the minimum achievable gap with respect to non-aromatic dyes. The second one, and most important, is the electron confinement within the rings, induced by the aromatic resonance stabilization, arising from the aromatic non-degeneracy of the ground state in polyarilenes. In fact, the two mesomeric forms (aromatic and quinoid) are not energetically equivalent in this class of

materials. Stabilising the less energetically favourable quinoid form via chemical modification of the polyaromatic backbone is a second way to reduce the gap.

Another contribution to the overall magnitude of the energy-gap, which applies to all conjugated materials, arises from the intermolecular interactions. Both the strength of these interactions and the geometrical arrangement of the conjugated segments in the aggregate or in the film[8] influence significantly the optoelectronic properties of the materials in general, and particularly the width of the energy-gap.[25b]

In a review paper published in 2007, Roncali[25b] presented a list of "synthetic tools", related to the factors discussed above, which are commonly employed by chemists for fine tuning of the energy-gap of conjugated materials. For instance, the insertion of one ethylene linkage between the aromatic rings of poly(*p*-phenylene) (PPP) or polythiophene (PT), to give poly(*p*-phenylenevinylene) (PPV) or poly(thienylenevinylene) (PTV), respectively, leads to a decrease of the overall aromaticity and to an increase of the molecular planarity, ultimately causing a reduction of the energy gap.[25b] However, the addition of two or more double bonds between the aromatic rings has the opposite effect, as the lower aromaticity and higher planarity are counteracted by the increased vibrational freedom of the molecular backbone.[25b]

To suppress both vibrations and rotations, conjugated systems can be rigidified by the addition of covalent bonds between the elemental aromatic moieties, as in the case of the ladder-type PPP,[26] with beneficial effects also on the luminescence efficiency of the oligomer/polymer. Materials exhibiting extreme molecular rigidity, extended electron delocalization, and therefore narrow energy-gap, are those based on fused-aromatic moieties[27]. The use of fused rings offers an additional benefit compared to the covalent fastening approach, as rings are usually selected and combined so as to increase the quinoid character of the aromatic moiety connected to the

main chain, thereby favouring a more extended electron delocalization and a narrower energy-gap.[25b]

The same effect can be obtained, via different synthetic routes, by introducing suitable electrophilic or nucleophilic groups in the conjugated system. In general, the introduction of electron-acceptor groups tends to stabilize the quinoid character of a molecule in the ground-state, with a concomitant narrowing of the gap as a result of asymmetric stabilisation of the HOMO and LUMO. Furthermore, electron-withdrawing groups also increase the ionization potential, thus making the neutral state of the compound more stable and less prone to degradation. The main drawback in this approach, however, is that polymerization processes relying on oxidation steps become more challenging.[25b]

The introduction of electron-donors, instead, leads mainly to an increase of the highest occupied molecular orbital (HOMO) energy (i.e. a reduction of the ionization potential), also resulting in a reduction of the energy-gap.[25b] A similar trend is observed also with the incorporation of heavier atoms in molecular backbone, such as selenium or tellurium instead of sulphur.[28] The resulting materials exhibit an overall narrowing of the energy-gap as a result of a destabilization of the HOMO, stabilization of the LUMO, and an overall decrease of the aromaticity.[28q] Expectedly, the downside with these approaches involving a destabilization of the HOMO is the stability of the neutral state of the molecule in ambient conditions.

In many cases, however, NIR emitting OS are based on an electron-donor (D) and electron-acceptor (A) alternated D-A structure, which leads to a broadening of both the valence and the conduction bands and a consequent narrowing of the energy-gap.[25b] In these materials, the emission originates from intramolecular charge-transfer states at a lower energy compared to the excited states localised on the monomer units.[28b, 29]. In analogy to the D-A strategy, emission from intermolecular charge-transfer states has also been exploited by Tregnago *et*

al.,[30] who reported NIR electroluminescence from exciplexes at polyfluorene/hexaazatrinaphthylene bulk heterojunctions.

A different approach to achieve NIR emission, which does not necessarily entail an extended electron delocalization, is the use of phosphorescent metal complexes. With respect to fluorescent dyes, phosphorescent ones leverage emission from the lowest excited triplet state, whose energy is lowered with respect to the singlet by the exchange coupling.[31]. However, as mentioned in the introduction, the use of materials containing heavy metals raises some concerns, mainly related to their toxicity and sustainability.

2.3.2 Increased tendency to aggregation quenching for low-gap materials

Extensively conjugated NIR moieties exhibit a higher degree of molecular planarity compared to OS with larger gap, thereby favouring a more significant formation of poorly emissive (H-type) aggregates[8] with respect to visible luminophores. Such an issue can be tackled by adopting the same well-established strategies employed for visible conjugated emitters. For instance, in the case polymers, aggregation quenching can be partially suppressed by increasing the molecular weight, but this works only so far, because beyond a certain point polymer chain kinks and geometric defects intervene to reduce the effective conjugation length, *i.e.* the length of the hypothetical oligomer whose lowest transition energy corresponds to the one of the polymer.[32]

In general, aggregation quenching can also be limited via molecular design,[2a] or by threading the emitter into cyclodextrin rings so as to form conjugated polyrotaxanes.[2b, 33] In most cases however, the approach that has been chosen in practice to limit undesired intermolecular interactions of NIR chromophores is that of a dilution in a solid state matrix, either via solution or vacuum processing,[6a, 34] in which the matrix acts both as “solid solvent” (and thus quenching inhibitor) and charge-transport agent. Alternatively, NIR moieties can be

copolymerised with a polymer host with a wider bandgap, with the additional benefit of reducing phase segregation.[28a, 35].

Interestingly, in terms of luminescence efficiency, the most successful approach to deal with aggregation effects is in fact not via suppression of the phenomenon but via exploitation of its potential in limiting non-radiative deactivation pathways of the excitations. This was introduced by Ben Zhong Tang and collaborators in 2001,[36] and later refined and extended to a large number of derivatives and analogues. Specifically, they demonstrated that some chromophores, when functionalized with freely rotatable peripheral aromatic rings, can form highly emissive aggregates in the condensed state, despite being relatively poor emitters in solution. This effect, aptly named "aggregation-induced emission" (AIE), is present mostly in luminogens that feature moieties with a propeller-shaped molecular structure, such as tetraphenylethylene. Such a structure sterically limits the π–π molecular stacking responsible for aggregation quenching, but also favours intramolecular rotations of the peripheral rings. For this class of materials such rotations constitute the preferential non-radiative deactivation channel when the chromophores are isolated, e.g. in dilute solutions,[37] and it is blocked effectively by the aggregation occurring upon film formation.

In the past decade, the functionalization with peripheral rings of a variety of chromophores, such as distyrylbenzene, fluorene, pentacene, and pyrene, proved to be a successful tool to promote the AIE mechanism and achieve higher photoluminescence efficiency in the solid state.[38] However, despite the success in the visible range, AIE in the NIR has been rarely demonstrated, with most of low-gap AIE luminophores emitting at most in the "far-red" (650 – 700 nm) spectral range.[39] The main reason for this is probably the presence of rotational disorder in AIE dyes, which limits the π-electron delocalization along the chain, and therefore increases the energy-gap with respect to molecules with a rigid molecular

backbone, as discussed in the previous section. Furthermore, to obtain "virtually pure" NIR emission, AIE dyes should have a longer π-conjugated backbone (vide infra), which would be more strongly protected from intermolecular interactions by the peripheral rings with respect to visible AIE luminophores.

2.3.3 The relation between energy gap and luminescence efficiency

Regardless of the success in controlling detrimental (H-type) or advantageous (AIE-type) aggregation effects, the so-called "energy-gap law" (E_G-law)[9] for radiationless transitions poses another intrinsic limitation to the efficiency of NIR chromophores. According to this the non-radiative rate of a fluorophore should increase exponentially as the energy gap is reduced, as a result of the increased overlap between the excited and the ground state vibrational manifolds. In principle, the problem could be circumvented by increasing the rigidity of the molecular structure, although this usually corresponds also to an increased molecular planarity, thus ultimately favouring H-type aggregation quenching.

Experimentally, the validity of the E_G-law has been tested in different works,[27a, 40] and we report in **Figure 3**, some examples from the relevant literature. An important caveat to note, however, is that the validity of the E_G-law can only be easily verified via comparative studies on compounds with similar chemical structure and composition, and different energy-gap. The crucial corollary following from such a caveat is that relatively high radiative efficiencies can still be obtained, via a careful molecular design, also from materials with narrow E_G, as demonstrated in some of the works reported in this review. For instance, in 2017 Ly et al. at the National Tsing Hua University (Taiwan) demonstrated phosphorescent NIR OLEDs emitting from 600 to 950 nm with efficiencies up to 24 %.[6b] Earlier this year, Kim *et al.* reported thermally activated delayed fluorescence OLEDs that operate in the 600 – 900 nm range with a maximum EQE of nearly 10% using a boron difluoride curcuminoid derivative. [6c] Later,

Minotto *et al.* demonstrated OLEDs incorporating purely fluorescent emitters with an emission above 900 nm peaking at 840 nm and exhibiting an unprecedented EQE of 1.15% for purely organic materials without leveraging triplet-assisted mechanisms.[6a]

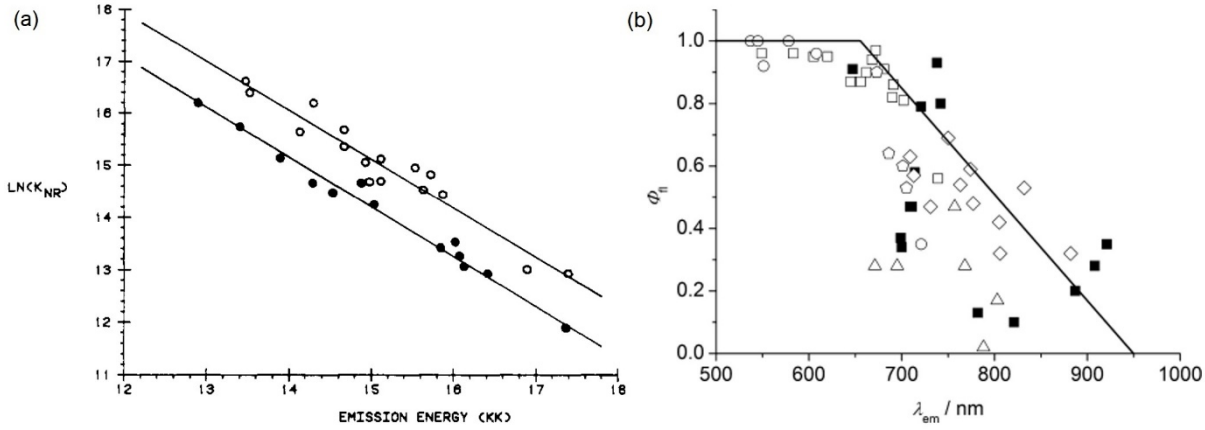

Figure 3. (a) Semilogarithmic plot of the non-radiative emission rate (K_{NR}) vs. the emission energy for the bis-2,2'-bipyridine (bpy) or 1,10-phenanthroline (phen) complexes of Os(II) [40a]. (b) Fluorescence quantum yield for fluorophores from different dye classes in relation to their respective emission wavelength. The black line illustrates the empirical trend found for the decrease of the fluorescence quantum yields in the NIR region.[41] All data for squaraines (black squares) originate from.[42] The other classes of dyes are rylene bisimides (open circles for perylene bisimides, open pentagons for terrylene bisimides), cyanine dyes (open triangles), BODIPY dyes (open squares), and PPCy dyes (open diamonds) the values of which were taken from the literature.

In the following, we will delve into the strategies that have been proposed so far to try and address the main challenges outlined above, highlighting in particular the successful ones that have led to the current state of the art. To this end, we structure our review by focusing on phosphorescent, fluorescent "triplet leveraging" (i.e. TADF/TTA), and "purely fluorescent" materials and related devices, as we consider this the most meaningful way also in relation to the potential fields of application and their requirements (e.g. in terms of toxicity, bandwidth, efficiency etc.).

3. OLEDs efficiency

The key parameter of an organic light-emitting diode is the external quantum efficiency, EQE, *i.e.* the ratio between photons emitted from, and unitary charges injected into, the device. This parameter can be further expressed as the product of the light out-coupling efficiency (ξ) and the internal quantum efficiency (IQE). Assuming only singlets and triplets as the possible radiative species (even though some results have lately also reported doublet emission, as mentioned in section 7 below), the latter can in turn be divided in a contribution due to emission from singlets (or fluorescence) and a contribution due to emission from triplets (or phosphorescence), so as to read:

$$EQE = \xi \cdot IQE = \xi \cdot \gamma \left[r_{st} \cdot \phi_{FL} + (1 - r_{st}) \cdot \phi_{PH} \right] \quad (1)$$

Where r_{st} is the singlet to total number of excitons ratio, ϕ_{FL} (ϕ_{PH}) is the fluorescence (phosphorescence) efficiency of the emitting layer and γ is a factor that takes into account the carriers populations imbalance (more precisely the ratio of minority to majority carrier populations). It is reasonable to assume, at least at 0th order, that ξ and γ have the same value for singlets and triplets. In practice, for the phosphorescence efficiency to be significant there must be significant spin-orbit coupling and thus intersystem crossing (ISC), so that most of the singlets will transfer to the triplet manifold in such cases during their lifetime. It is thus theoretically possible to harvest all singlets and triplets, and achieve nearly 100% IQEs, for materials with unit photoluminescence quantum yield and devices with balanced populations.[43] This intrinsic advantage of phosphorescent OLEDs with respect to fluorescent ones is counter-balanced by a number of potential shortcomings, such as the need to use heavy (mostly toxic) metals to induce spin-orbit coupling and thus effective ISC, by a typical roll-off of the efficiency versus current characteristics at high current densities (mainly due to saturation

of the few, because of the need of solid-state dilution, but comparatively long-lived triplet sites), and by the need to include in the device architecture exciton blocking layers to limit exciton diffusion to the electrodes where they can be quenched effectively.

The parameters ξ and γ are strongly affected by the device architecture. For example, the improvement of ξ (usually limited to 20% in OLEDs fabricated on top of indium-doped tin oxide, ITO, as calculated from Snell's law) is mainly related to the engineering of the refractive index, although it also depends on the orientation of the actual emissive chromophores, that in turn is not trivial to control.[44]

Turning to the factor accounting for the populations balance, γ, this can be influenced by either device or materials structure. The most common strategies adopted to balance the carriers population have often relied on insertion of *ad-hoc* hole/electron-injection, hole/electron-transport, or even hole/electron *blocking* layers at the relevant interfaces, most commonly between the electrodes and the emitting layer,[45] but in some cases also in the middle of the device.[46] Combination of donor and acceptor moieties via covalent linkages to the main emitting material has also been explored in attempting to balance hole and electron injection/transport, and thus their populations.[47]

The luminescence efficiency (or quantum yield, ϕ_{PL}) without explicitly differentiating between fluorescence and phosphorescence, and r_{st} are strongly related to the intrinsic properties of the emitters. In particular, for NIR emitters, ϕ_{PL} is affected by the aforementioned energy-gap law and aggregation quenching. Simple spin statistics arguments suggest instead that $\boldsymbol{r_{st}}$ is limited to 25% maximum, and these are experimentally supported.[48] Results consistent with a higher singlets/triplets ratio than suggested by simple statistics arguments had been reported in the past,[24b] but these would appear to still be consistent with the 25%

maximum (initial) singlet formation efficiency if triplet-triplet annihilation (TTA) and thermally activated delayed fluorescence (TADF) effects were to be taken into account.[49]

4. Phosphorescent NIR OLEDs

In order to induce effective spin-orbit coupling and thus enable radiative transitions from the excited triplets to the ground state (as well as intersystem crossing from the singlet to the triplet manifold) heavy metals are commonly used. It is just natural then to start reviewing NIR electrophosphorescence by separating results obtained via use of lanthanides (Section 4.1) and transition metals (Section 4.2). However, we also reserve a subsection to phosphorescent porphyrins, as the number and importance of results obtained by utilisation of these materials warrants a separate mention. We also dedicate a final subsection to the new approach based on singlet fission to generate triplets. This is particularly interesting for the NIR, given the energies involved (both for singlets and triplets), and because it enables IQEs over 100 %.

Table 1. NIR PL peak, Quantum Yield (ϕ_{PL}), NIR EL peak and Max EQE of the most important class of materials leveraging the phosphorescence mechanism.

Class	Atom	NIR PL peak [nm]	ϕ_{PL} [%]	NIR EL peak [nm]	Max EQE [%]	Year/reference
Lanthanide	Er	1522	N/A	1533	N/A	1999[50]
	Er	1540	N/A	1540	N/A	2000[51]
	Nd	890	0.07	890	8 mcd/A	2001[52]
	Yb	977	N/A	977	0.001	2001[53]
	Os	731	4.0	718	1.5	2009[54]
	Os	805	0.2	814	2.7	2009[54]
Ir complex	Ir	720	N/A	720	0.25	2006[55]
	Ir	765	17.0	760	4.5	2017[56]
	Ir	710	16.0	714	3.07	2017[57]
	Ir	775	6.0	775	0.5	2015[58]
	Ir	777	3.6	780	2.2	2013[59]
Pt complex	Pt	740	81.0	740	24	2017[6b]
	Pt	705	31.0	705	10.5	2007[60]
	Pt	720	24.0	720	8.5	2007[60]
	Pt	760	80.0	772	8.5	2007[61]
	Pt	760	80.0	765	6.3	2007[62]
	Pt	842	22.0	848	2.8	2016[63]
	Pt	883	22.0	886	3.8	2016[64]
	Pt	773	35.0	773	8.0	2011[65]
	Pt	891	15.0	900	3.8	2011[65]
	Pt	1022	8.0	1005	0.12	2011[65]

4.1 Lanthanide-based materials

Since the late 1990's, the first attempts to achieve near-IR light-emitting diodes exploited rare-earth metal complexes, for instance lanthanide complexes such as Er(III), Yt(III) and Nd(III). These complexes are well known for their NIR phosphorescent properties in the 800 to 1600 nm spectral range, that is useful for potential applications in bioscience and telecommunication, such as bioimaging, planar waveguide amplifiers, and organic light-emitting diodes (OLEDs).[66] In such a class of rare-earth metal complexes, phosphorescence

arises as a narrow NIR emission band originating from the 4f states of the central ions, which are excited via intramolecular energy transfer from the triplet-excited states of the ligand.[67]

Different methods have been developed to enhance the luminescence efficiencies from lanthanide complexes, that can be used as neat emitters, in blends with an efficient charge/energy transport host materials, or copolymerized covalently to a polymer main chain.[51, 53, 68] The first remarkable attempts to achieve a "purely" NIR phosphorescent OLED (with 100% emission in the NIR region) are those by Curry and Gillin in 1999, by incorporation of an erbium-doped material, i.e. erbium (III) tris,8-hydroxyquinoline (ErQ), as a neat emitting layer in multi-stack OLEDs exhibiting electroluminescence at 1.54 μm at room-temperature.[50, 69] However, more efficient NIR electroluminescence from OLEDs incorporating lanthanide complexes have been achieved by blending this class of complexes in a host matrix. Frequently used host materials include poly[2-methoxy-5-(2-ethylhexyloxy)-1,4-phenylenevinylene (MEH-PPV, with emission peak at 550 nm), poly(N-vinylcarbazole) (PVK , emitting at 450 nm) and poly(dioctylfluorene-alt-benzothiadiazole) (F8BT, emitting at 550 nm). The related chemical structures are shown in **Figure 4**.[51-53, 70]

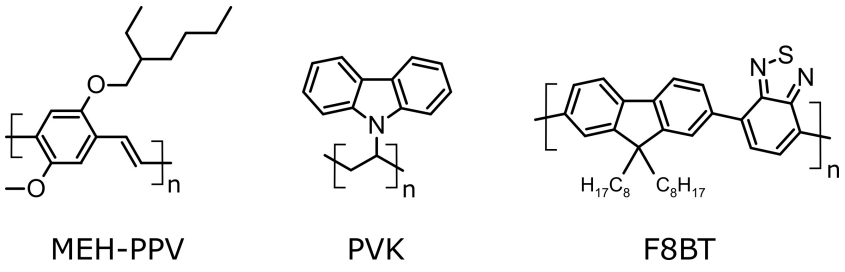

Figure 4. Chemical structures of most used host materials: MEH-PPV (emission peak ~ 625 nm), poly(N-vinylcarbazole) (emission peak ~ 450 nm, PVK) and poly(dioctylfluorene-alt-benzothiadiazole) (emission peak ~ 550 nm, F8BT).

In 2000, Sun et al. investigated the PL and EL properties of another erbium complex, tris(acetylacetonato)(1,10-phenanthroline)erbium [Er(acac)3(phen)], blended at 80 wt% with PVK as the host-material (1.54 μm emission with an ITO/PVK:Er(acac)3(phen)/Al:Li/Ag structure).[51] Later, Slooff et al. reported luminescence at ~ 890 nm from a lissamine-functionalized terphenyl-based neodymium complex (Ls.Nd^{3+}) blended at 10 wt% with F8BT. Although the lissamine dye is not commonly used to achieve NIR emission, lissamine shows a higher triplet population under electrical excitation than that under optical excitation, and therefore acts as key enabler of the NIR emission from the Nd^{3+} complex.[52]

In the same year, Harrison and collaborators reported the study of phosphorescent OLEDs incorporating the lanthanide complexes Yb(TPP)acac (EL peaked at 977 nm) or Er(TPP)acac (EL peaked at 1560 nm), where TPP is 5,10,15,20-tetraphenylporphyrin and acac is acetylacetonate. The lanthanide complexes were blended with MEH-PPV or bis-alkoxy-substituted poly(p-phenylene), PPP-OR1. MEH-PVV was selected since the TPP ligand exhibits a good spectral overlap between its Q-absorption bands and the MEH–PPV fluorescence, thereby promoting efficient Förster energy transfer. However, PPP–OR11 showed an even better spectral overlap with the Soret band of the TPP ligand than that observed with MEH-PPV. Thanks to this, they achieved a five-fold higher EL efficiency with respect to MEH-PPV OLEDs (reaching up to 0.001 %, with an applied bias of 7 V) at 977 nm by incorporating the PPP–OR11:Yb(TPP)acac active blend in a device. Interestingly, the turn-on voltage of such devices was as low as 4 V, one of the lowest reported at that time.[53]

4.2 Transition metals-based materials

Highly emissive NIR Ir(III) and Pt(II) complexes, incorporated as dopants in a host matrix, have also been widely investigated in the early 2000s.[3, 71] One of the first successful attempts to achieve a purely NIR emission from an OLED incorporating Ir(III) complexes was

reported by Williams et al. in 2006. The authors obtained NIR electrophosphorescence peaked at 720 nm from the Ir(III) bis(1-pyrenyl-isoquinolinato-*N,C'*) acac (referred to as NIR1) complex, blended with a PVK and pyrrolobenzodiazepine (PBD) matrix. From such a blend, they achieved an EQE of 0.25% and an output radiance of 100 μW/cm^2.[72]

Alternatively, Tsuzuki and collaborators demonstrated phosphorescent NIR OLED by exploiting different Ir(III) complexes acting as host and guest. More precisely, they chose tris(1-pheny-lisoquinolinolato-C^2,*N*)Ir(III), Ir(piq3), as a red phosphorescent dopant and bis(2-phenylpyridinato-*N*,C^2')Ir(III)(acac), (ppy)2Ir(acac) as a host material. The green emission of the (ppy)2Ir(acac) host was efficiently quenched at low concentrations of Ir(piq)3, indicating that the triplet excitons generated in (ppy)2Ir(acac) are efficiently transferred to Ir(piq)3. OLEDs incorporating (ppy)2Ir(acac) doped with 0.3 wt% Ir(piq3) exhibited EL peaked at 640 nm (with ~ 20 % of the emission above 700 nm) and an EQE of 9.2%.[73]

More recently, Xue and collaborators reported highly efficient NIR phosphorescent OLEDs (with emission over 750 nm) with a low roll-off of the EQE by exploiting NIR-emitting so-called "homoleptic" (i.e. with all identical ligands to the metal) facial isomers of Ir(III) octahedral complexes. The authors fabricated OLEDs by blending such emitters in an indolocarbazole-triazine-based matrix, whose emission largely overlaps with the absorption of the Ir(III) complexes. Thanks to this, NIR-OLEDs incorporating a blend with 1 wt% of Ir(III) complex exhibited virtually pure NIR EL peaked at 760 nm, with an EQE of 4.5 % and a remarkable maximum output radiance of 45 W m^{-2}.[56]

Yet more efficient NIR OLEDs (currently state-of-the-art) were reported by Tuong Ly and collaborators[6b] by exploiting a new series of 2-pyrazinylpyrazolate Pt(II) complexes (1-4 shown in **Figure 5**). Among those, complexes 1, 2 and 3, show a PL quantum yield ϕ_{PL} of 81% (with PL peaked at 740 nm), 55% (PL peaked at 703 nm) and 85% (PL peaked at 673 nm),

respectively. Such an efficient NIR luminescence is mainly due the ordered solid-state packing arrangement, attributed by the authors to the edge-on preferred orientation in the vacuum-evaporated thin films, in turn detected by combining photophysical data, wide-angle X-ray scattering, angle-dependent luminescence and computational modeling. This feature likely promotes exciton-like emission among the molecular aggregate and along the d_z2 orbital, which efficiently suppresses coupling between the exciton and the optical phonon. The OLED architecture has also been optimized by using different hole-injecting materials and layers (HILs), hole-transporting layers (HTLs), or electron-transporting layers (ETLs), and electron-injecting layers (EILs) to favour exciton formation and recombination inside neat Pt(II) complex-based active layers. OLEDs incorporating complex 1 in **Figure 5** showed the highest EQE (24%) reported so far with an EL peaked at 740 nm. Furthermore, 78% of such emission falls in the NIR, resulting in a (purely) NIR EQE of 19.1 %, and excellent maximum radiance values.[6b]

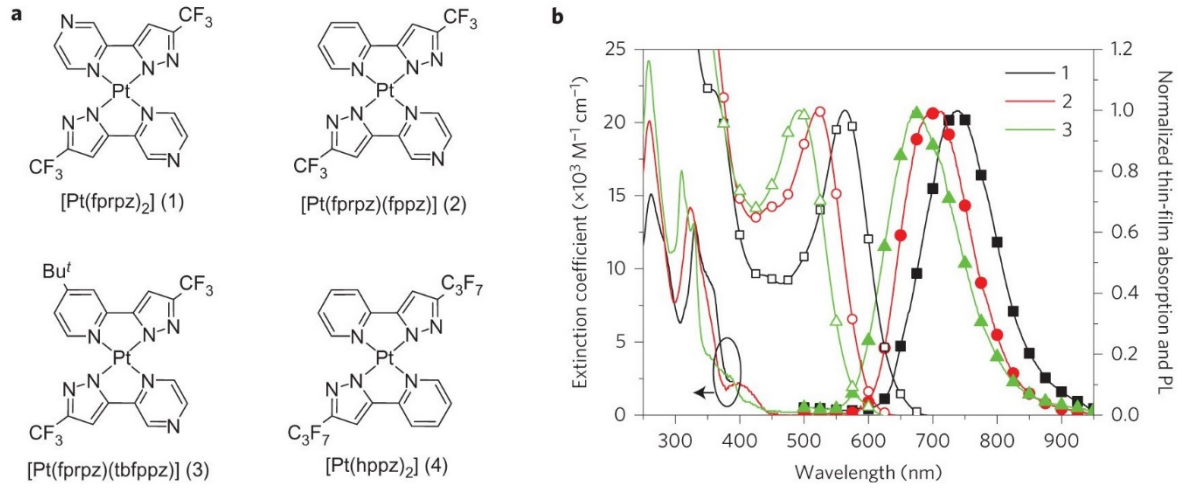

Figure 5. Chemical structure and optical properties of Pt(II) complexes 1–3. a, Pt(II) complexes 1–3. Structurally characterized [Pt(hppz)2] (4), whose packing arrangement was used to simulate the dimer and trimer of 1 in the solid state is also shown. b, The absorption spectra of 1–3 in THF. The corresponding absorption (unfilled symbols, righthand y axis) and emission spectra in solid film (filled symbols, righthand y axis) normalized at the peak wavelength are also shown.[6b]

4.3 Porphyrin-based (phosphorescent) materials

Another promising class of complexes which merits separate attention is that of porphyrins that can coordinate a metal via the lone pairs of the nitrogen pyrrolic rings. Depending on the coordinated metal, either phosphorescent or fluorescent emission is possible, but we will concentrate here on phosphorescence, and review NIR fluorescent porphyrin devices in Section 6 below.

Within this context, particular emphasis has been placed on the Pt-based porphyrins.[34c, 63, 74] Pt-based porphyrins have been widely investigated due to the intense absorption and emission in the red-to-NIR region.[3, 75] Although the first reported OLEDs incorporating Pt-porphyrins as emitters did not exhibit EL above 650 nm,[3, 76] Forrest and collaborators were able to obtain EL peaked at 772 nm and an EQE of ~ 8.5% in 2007, by exploiting a Pt–tetraphenyltetrabenzoporphrin [Pt(tpbp)]) as a dopant in a tris(8-hydroxyquinoline) aluminum (Alq_3) matrix,[61] and improved device design in the form of a bathocuproine (BCP), hole-exciton blocking layer, and a lower dye concentration (thus reducing aggregation quenching) with respect to their own previous results (EQE of 6.3%).[74c]

Further results of efficient EL above 800 nm from porphyrin derivatives have followed in subsequent years. Decoration of the pyrrolic rings on the porphyrins with conjugated systems of various extents (such as benzene fused rings), has been successfully used to extend emission further into the NIR. Schanze and collaborators for example reported OLEDs incorporating Pt-tetraphenyltetranaphthoporphyrin [Pt(tptnp)] as dopant in a 4,4-bis(*N*-carbazolyl)-1,1′-biphenyl (CBP) matrix in 2009. Such devices exhibited a maximum EQE of ~ 3.8 % and a maximum radiance of 1.8 mW/cm^2 peaked at 896 nm.[74b] In 2011 they further extended and improved on such results (EQE up to 9.2% at 770 nm) by exploiting a family of Pt-tetrabenzoporphyrins with extended conjugation, as shown in **Figure 6**, and emitting from 770 nm to 1010 nm.

Interestingly, those emitters have been investigated both in OLEDs in blend with either Alq_3 or CBP, and in polymer LEDs (PLED) with PVK and PBD.[34c] More recently (2016), Jian Li and collaborators at Arizona State University were able to obtain EL at 848 and 846 nm, with EQE of 2.8% and 1.5% respectively by leveraging Pt-azatetrabenzoporphyrin complexes, PtNTBP and cis-PtN2TBP.[63]

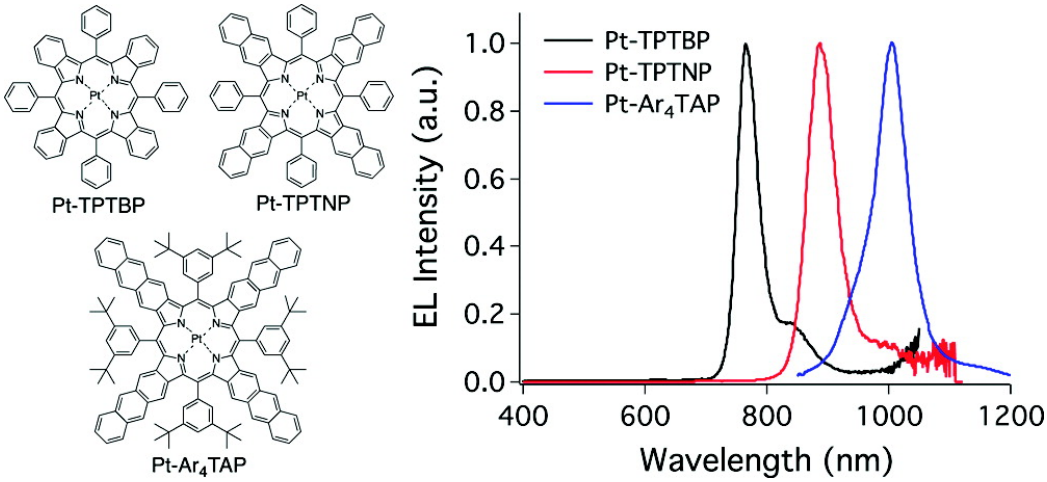

Figure 6. Chemical structures of Pt-TPTBP, Pt-TPTNP, and Pt-Ar4TAP and the corresponding electroluminescence spectra of the Pt-porphyrin PLEDs consisting of 2% (by weight) of the chromophores in a PVK:PBD (6:4) host.[77]
Reproduced with permission.[77] Copyright 2011, American Chemical Society.

Copolymerisation of Pt-porphyrin with host semiconducting polymers have also been exploited recently,[78], in analogy to what reported previously (early 2000s, see below) for metal-free fluorescent porphyrins.[79] Freeman et al. tested four conjugated copolymers containing different loading (0.5, 1, 2 and 5 %w/w) of dimesityl diphenyl porphyrin platinum, MPP(Pt), into the host poly(9,9-di-n-octylfluorenyl- 2,7-diyl) (PFO) backbone. By incorporating these polymers in PLEDs as neat emitting layer, the devices exhibit an EL peaked at 665, 736 and 818 nm, with EQE up to 0.48%.[78] Freeman et al. in 2016 applied a similar synthetic method by copolymerising the same Pt-porphyrin with diphenylanthracene.[35c]

PLEDs incorporating such a copolymer exhibited EL spectra peaked at 666 nm and 760 nm, featuring a maximum EQE of 0.3%.[35c]

4.4 NIR phosphorescence via singlet fission

The main advantage of using phosphorescent materials as emitters in OLEDs is the radiative exciton production efficiency, which can be up to 100 %. However, leveraging of singlet fission into a pair of triplets (only for materials for which triplet energy is ~ half that of the singlet) may enable even higher efficiencies. Singlet fission has been actively investigated primarily as a means to increase the efficiency of photovoltaic diodes (PVDs),[80] but it lends itself to NIR electroluminescence as well, because the energy of the resulting triplet excitons is likely to fall in the NIR range, being approximately half that of the singlet. Although triplet emission from the materials best suited for singlet fission might not be particularly efficient at room temperature, it is possible to efficiently harvest these triplets by using such materials (typically acenes, such as tetracene, rubrene, pentacene) via a sensitization scheme. For example, this has been reported in a recent paper by Adachi and collaborators.[81] They fabricated OLEDs featuring as active layer a blend of rubrene as the host and singlet-fission sensitizer, and the NIR phosphorescent erbium(III) tris(8-hydroxyquinoline) complex as the triplet-harvester and emitter. From such OLEDs, they successfully obtained NIR EL peaking at 1530 nm and measured an exciton production efficiency of 100.8 %.

5. Leveraging triplets for fluorescent NIR emission: TADF and TTA

While the intrinsic singlet formation rate is limited to 25% of the total number of excitons formed according to simple spin statistics arguments, the proportion of singlets can increase following two distinct processes that can convert triplets into singlets. The first and probably

most important is via reverse intersystem crossing (rISC) (**Figure 7**), which then leads to the so-called thermally activated delayed fluorescence (TADF).[82]

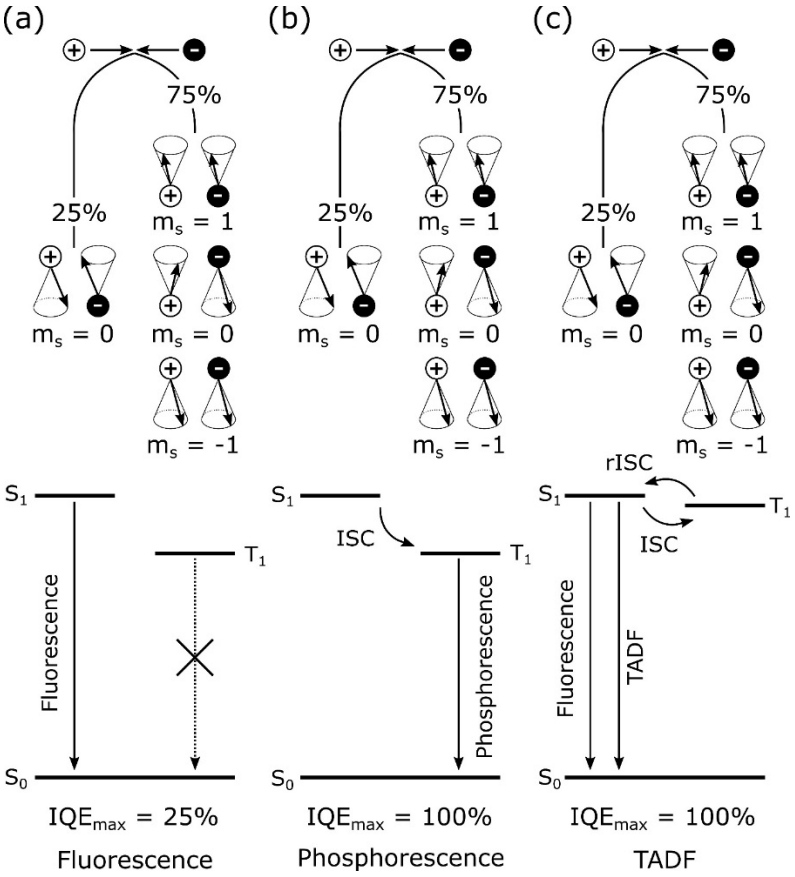

Figure 7. Schemes of the three main radiative mechanisms in OLEDs.

This process requires small (compared to the thermal energy) values of the exchange energy (difference between singlet and triplet energies, ΔE_{ST})), and is generally expected to show a strong temperature dependence, and can in principle lead to nearly unitary IQEs (provided the fluorescence efficiency is also ~ 1, Figure 7c).[82] As a result, devices featuring TADF exhibit maximum EQE values comparable to those obtained by the best performing phosphorescent OLEDs, with the additional benefit of being metal-free.[83]

Alternatively, triplet-triplet annihilation (TTA) can also be responsible for singlet regeneration and thus for boosting the EL efficiency.[49, 84] Clearly, as two triplets are required to generate a singlet via this route the maximum efficiency can never exceed 62.5% (i.e. 25+75/2 %) of the quantum yield of the emitting material, for this mechanism even under the (ideal) assumption that the entire triplet population undergoes TTA. For these reasons, efforts have so far mostly concentrated on exploitation of TADF, rather than TTA, and we also focus on TADF emitters (in the far red and NIR region) in what follows.

5.2 TADF materials as NIR emitters

A general strategy that has been pursued to obtain molecules and polymers with small exchange energies[85] is to combine electron-donor (D) and electron-acceptor (A) moieties, to favour the formation of intramolecular charge-transfer (ICT) excited states, in which the overlap between the HOMO and LUMO orbitals is minimal. This is usually achieved by spatially separating D and A with an aromatic bridge and/or by twisting the D and A along the D-A axis.[82b, 86]

Focusing on the NIR spectral region, however, only few works so far have reported NIR TADF-based OLEDs with EQE exceeding 5 %, as shown in **Table 2**.[6c, 39b, 87] This is mainly due to the fact that the poor overlap between HOMO and LUMO orbitals not only leads to a reduction of ΔE_{ST}, but also to lower radiative rates. While for visible emitters with large energy-gap this represents a minor issue, for TADF NIR emitters the low radiative rates have a detrimental effect on the fluorescence efficiency (ϕ_{FL}), due to the concomitant increase of the non-radiative rate imposed by the E_G-law.

Because of the E_G-law, the best performance from OLEDs incorporating TADF narrow-gap emitters has been obtained more in the deep-red spectral region than in the NIR, with electroluminescence (EL) maxima peaked at ~ 700 nm or shorter wavelengths. The first deep-

red TADF OLED with EQE beyond 5 % and EL maximum at 668 nm was reported in 2015 by Wang et al.,[39b] who fabricated devices having as emitting layer blends of 1,3,5-tris(*N*-phenyl-benzimidazol-2-yl)benzene (TPBi) and TPA-DCPP (TPA=triphenylamine; DCPP=2,3-dicyanopyrazino phenanthrene), acting as host and emitting guest, respectively. They obtained a record EQE of 9.8 % by leveraging rISC, and thereby TADF, afforded by the 0.13 eV ΔE_{ST} of the V-shaped D–π–A–π–D TPA-DCPP compound, with DCPP as the electron acceptor, DPA as the electron donor. Furthermore, Wang et al. demonstrate that TPA-DCPP is also an AIE-active material, a feature that further boosts the ϕ_{FL} in the solid-state emitting layer.

Table 2. NIR PL peak wavelength, Quantum Yield (ϕ_{PL}), NIR EL peak wavelength and Maximum EQE of the most important class of materials leveraging the TADF strategy.

Molecule Design	NIR PL peak [nm]	ϕ_{PL} [%]	NIR EL peak [nm]	Max EQE [%]	Year/reference
D-A-D	708	14	668	9.8	2015 [39b]
D-A-D	716	57	716	8.53	2018 [88]
D-A-D	721	70	721	9.69	2018 [88]
D-A-D	730	52	730	8.09	2018 [88]
D-A-D	743	26	743	2.03	2018 [88]
D-A-D	750	22.5	750	1.44	2018 [88]
D-A-D	771	7.5	771	0.34	2018 [88]
D-A-D	782	3.5	782	0.27	2018 [88]
D-A	756	13	777	2.19	2017 [89]
D-A	687	63	698	10.19	2017 [89]
D-A	-	0.3[a)]	970[a)]	0.1[a)]	2017 [90]

[a)] In this work, the TADF material was used as host in blend with a NIR phosphor.

To shift the EL further towards the NIR, in 2017 Yuan *et al.*[87] synthesised a similar TADF compound (APDC-DTPA), having the same wedge-shaped D–π–A–π–D structure as TPA-DCPP but with acenaphtho[1,2-b]pyrazine-8,9-dicarbonitrile (APDC) as acceptor unit,

which has a stronger electron-withdrawing ability compared to the DCPP moiety used by Wang. By blending APDC-DTPA with TPBi, they achieved EQEs up to 10.19% with EL peaking at 693 nm. In addition, in another recent work the same group[91] demonstrated that the emission of APDC-DTPA OLEDs can be bathochromically shifted up to 728, while retaining an EQE > 5 %, by blending the TADF emitter with different hosts exhibiting a stronger molecular dipole moment compared to the previously employed TPBi, such as the organometallic bis[2-(2-benzothiazolyl-*N*3)phenolato-O]zinc ($Zn(BTZ)_2$). Namely, hosts with higher polarity like ($Zn(BTZ)_2$) offer a better solid-state solvation of D – A TADF emitters exhibiting strong ICT characteristics, with the twofold benefit of increasing the fluorescence efficiency (ϕ_{FL}) and at the same time shifting the emission into the NIR region.

In the same spectral range, early this year Kim et al.[6c] reported an EQE of 10 % and EL maximum at 721 nm from OLEDs incorporating an active layer based on a CBP host blended with a D–A–D TADF curcuminoid derivative consisting of two triphenylamine groups and one acetylacetonate boron difluoride acceptor (shown in **Figure 8**). In contrast to previously reported twisted D–A TADF emitters, Kim *et al.* demonstrated that such a curcuminoid derivative exhibits a strong overlap between the hole and electron wavefunctions involved in the optical transition responsible for the NIR emission, thereby leading to a large oscillator strength. Such a feature, combined with a non-adiabatic coupling effect between the low-lying excited states, allowed them to obtain not only high-efficiency NIR emission, but also low-threshold (7 μJ cm^{-2}) amplified spontaneous emission (ASE) from the TADF curcuminoid doped CBP films.

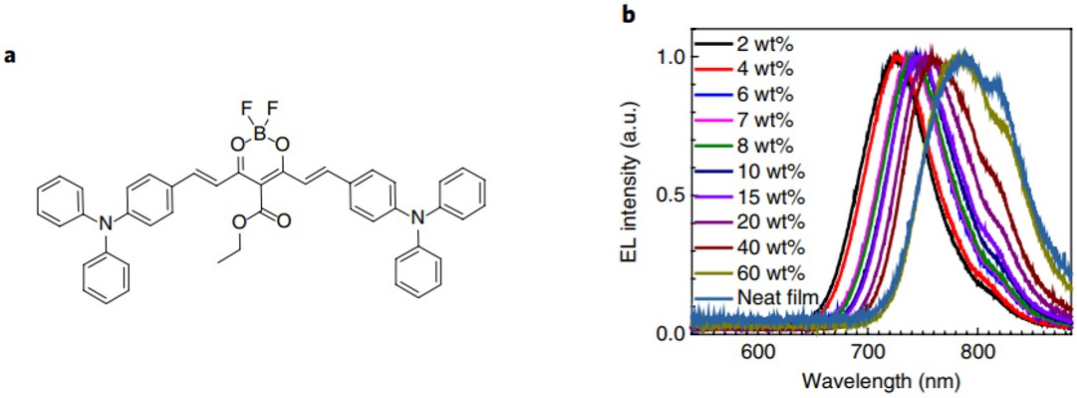

Figure 8. a) Chemical structure of the NIR-emitting curcuminoid derivative. (b) EL spectra in OLEDs based on an emitting layer containing a CBP host blended with boron difluoride curcuminoid derivative at different doping concentrations.[6c]
Adapted with permission.[6c] Copyright 2018, Springer Nature.

5.3 TADF materials as triplet sensitizers

Despite the very promising achievements obtained in the 670 – 730 nm (deep-red/NIR) spectral range, with EQE values reaching up to 10 %, much lower efficiencies have been reported from TADF OLEDs emitting beyond 730 nm. Furthermore, TADF emitters usually exhibit broad emission spectra (~ 100 nm), discouraging their use for applications in which a high colour purity is required. To address such limitations, some authors have recently proposed an alternative strategy. Namely, TADF compounds can be used also as hosts or triplet sensitizers in combination with non-TADF emitters.[83b, 92] In such blended systems, up to 100 % of the excitons generated in the TADF host, including triplets harvested via rISC, can be resonantly transferred to a fluorescent or phosphorescent dopant emitting in the NIR. Indeed, the use TADF compounds as hosts or assistant dopants in combination with non-TADF emitters has already proved to be successful in the red spectral region, with EQE values approaching 20 %.[83b] With the TADF triplet-sensitization method, Adachi and collaborators[93] have recently demonstrated EL peaking up to 1100 nm from blends of 2-phenoxazine-4,6-diphenyl-1,3,5-triazine (PXZ-TRZ) as TADF host and copper phthalocyanine (CuPc) and platinum

phthalocyanine (PtPc) as NIR phosphors. Thanks to the efficient up-conversion of triplets into singlets via rISC in the PXZ-TRZ host, Adachi et al. showed that almost 100 % of the excitons generated in the active layer are used to obtain NIR phosphorescence. Although the relatively low phosphorescence efficiency ϕ_{PH} of the metal phthalocyanines did not allow them to obtain EQE values higher than 0.1 %, Adachi et al. suggest that such a hurdle could be overcome by using highly emissive NIR-phosphors.

6. Fluorescent NIR OLEDs

Compared to TADF and phosphorescent materials, fluorescent ones do not harvest triplet excitons (r_{st} = 25% and ϕ_{PH} ~ 0 at room temperature), and therefore their maximum IQE is limited to 25%, according to Equation 1. For this reason, and because of the concomitant action of the energy-gap law, the maximum EQE values of NIR fluorescent OLEDs reported so far did not exceed 2%. However, as mentioned before, fluorescent dyes are "heavy-metal-free", and therefore more environmentally sustainable and more appealing for applications in which biocompatibility is an issue compared to phosphorescent materials. Furthermore, exciton recombination dynamics in fluorescent chromophores are of the order of few nanoseconds, i.e. at least 100 times faster compared to both TADF and phosphorescent emitters, therefore ideal for Li-Fi applications aiming to reach transmission rates up to the Gb/s regime.[10]

In the following, we will review different classes of fluorescent emitters, starting from fluorescent porphyrins (Section 6.1) and polymers/oligomers incorporating heavy atoms (Section 6.2). However, the most efficient NIR fluorescent OLEDs have been obtained by leveraging D-A polymers (Section 6.3) and D-A-D or A-D-A oligomers (Section 6.4). Some of these chromophores benefit also from the AIE-effect, and we dedicate Section 6.5 to review the best results obtained from NIR OLEDs leveraging this effect. Finally, in Section 6.6, we report

some further achievements obtained from other families of NIR fluorophores that are not commonly employed as light-emitters in OLEDs, such as carbon nanotubes and squaraines.

6.1 Porphyrin-based (fluorescent) materials

The first fluorescent OLEDs incorporating conjugated semiconductors as active materials have been reported in the late 80s,[1] but the first NIR fluorescent OLEDs were reported only in 1995 by Baigent et al..[94] Such OLEDs, incorporating a cyano-substituted thienylene phenylene vinylene copolymer, exhibited EL peaked at 740 nm with an EQE of 0.2 %. However, following to this first report, some researchers found that fluorescent porphyrin derivatives, in analogy to phosphorescent ones, could be integrated as NIR emitters in OLEDs, typically copolymerized or in blend with a fluorescent host. The most important achievements have been reported in **Table 3**.

In 1999, Iqbal et al. [95] fabricated OLEDs showing higher EL efficiencies by leveraging a novel series of porphyrin-doped PPV-copolymers. Those copolymers consisted of an MEH-PPV polymer backbone functionalised with different loadings of tetraphenylporphyrin (TPP) as side groups. This approach of grafting the dyes to the polymer chain was investigated to address phase separation and aggregation quenching, the main issues affecting the efficiencies of the emitting materials in the solid-state blends. OLEDs incorporating such copolymers exhibited an emission peaked at 660 nm and 730 nm with EL efficiencies up to 0.56%.[79a, 95]

Alternative porphyrin-based structures have been designed by Ostrowski et al., who characterized the electroluminescence properties of a series of ethyne-bridged oligo[(porphinato)zinc(II)] species in blend PVK and MEH-PPV. Thanks to the ethyne bridging units, the authors were able to modulate the ground- and excited-state inter-chromophore electronic interaction, and therefore red-shift the PL and EL emission of such complexes from

the red to the NIR. OLEDs incorporating [(porphinato)zinc(II)] oligomers exhibited efficiencies up to 0.3% and emission in the 700-800 nm spectral range.[96]

Table 3. NIR PL peak wavelength, Quantum Yield (ϕ_{PL}), NIR EL peak wavelength and Maximum EQE of the most important class of materials leveraging the fluorescence strategy.

Class	Molecule Design	NIR PL peak [nm]	ϕ_{PL} [%]	NIR EL peak [nm]	Max EQE [%]	Year/reference
Copolymer	Porphyrin	725	3.3	730	0.56	2000[97]
	Porphyrin	720	9.0	720	0.3	2003[96]
	D-A	890	N/A	895	0.09	2015[28a]
	D-A	1000	N/A	990	0.02	2015[28a]
	D-A	708	15.0	680	0.48	2017[98]
	D-A	874	6.0	880	0.15	2017[98]
	D-A	840	17	840	1.15	2018[6a]
	D-A	713	5	708	0.15	2005[28p]
	D-A	734	22	723	0.30	2005[28p]
	D-A	754	9	744	0.05	2005[28p]
	D-A	770	9	759	0.20	2005[28p]
	D-A	790	1	790	0.02	2005[28p]
	D-A	740	4	740	0.2	1995[94]
Oligomer	Porphyrin	820	13.0	820	0.1	2011[99]
	Porphyrin	882	7.0	883	0.1	2011[99]
	D-A-D	1080	5.8	1080	0.28	2008[11]
	D-A-D	1255	N/A	1220	N/A	2008[11]
	D-A-D	725	7.0	725	0.28	2011[100]
	A-D-A	720	20	720	1.10	2017[34e]
	D-A-D	730	22	730	0.65	2013[101]
	D-A-D	N/A	N/A	760	1.9	2013[102]
	D-A-D	1035	N/A	970	0.05	2004[103]
SWCNT	-	1177	0.11	1177	0.01	2018[104]

With a similar approach, in 2011 Fenwick and collaborators investigated a linear meso-butadiyne-linked porphyrin hexamer (referred to as P6) and a cyclic one bound to a hexapyridyl template (c-P6T) to demonstrate an innovative approach to shift the fluorescence further into the NIR, either by leveraging the extended conjugation length of P6 or the curved π-surface of c-P6T.[34d] P6 and c-P6T were incorporated in a F8BT matrix, and used as active materials in solution-processed OLEDs. The nanoring complex c-P6T showed significantly red-shifted electroluminescence (peaking at 960 nm) compared to the linear hexamer (EL maximum at 883 nm). Both hexamers exhibited relatively low EL EQE (0.024 % and 0.009 % for c-P6T and P6, respectively). However, with the addition of the 4-benzylpyridine (BP) metal-coordinating ligand to the linear hexamer, the EL EQE increased by order of magnitude with respect to the uncoordinated P6:F8BT OLEDs, reaching up to 0.1%.[34d] Fenwick et al. attributed such a tenfold increase of the efficiency to the reduced intermolecular interaction between the porphyrin rings, and therefore suppressed aggregation quenching in P6BP:F8BT blends, thanks to the steric hindrance provided by the BP Zn-coordinating additive.

6.2 Fluorophores incorporating heavy-atoms

As mentioned in Section 2.3, a promising route to extend further the emission in the near-infrared region is the replacement of sulphur with heavier atoms in the molecular backbone, such as selenium or tellurium.[28a, 28c, 28e-p] Yang reported in 2005 a novel series of semiconducting conjugated D-A-D copolymers, having 9,9-dioctylfluorene as donor units and either 4,7-diselenophen-2¢-yl-2,1,3-benzothiadiazole (SeBT) or 4,7-diselenophen-2¢-yl-2,1,3-benzoselenadiazole (SeBSe) as acceptor groups. The optical band gap of such copolymers is 1.87 eV for SeBT and 1.77 eV for SeBSe, respectively. Interestingly, the copolymer optical gap based on SeBSe significantly decreases by adding few moieties (1%) in the D-A-D structure, from 2.92 eV (pure polyfluorene) to 1.78 eV. The PL emissions of such copolymers are peaked

at 734-790 nm, featuring quantum yields ranging from 1% (at 790) to 22% (at 734 nm). OLEDs incorporating those emitters exhibited quantum efficiencies up to 0.3% with EL peaking at 723 nm, although the EL efficiency decreased to 0.02 % at increasing SeBSe loading.[28p] The same maximum EQE (0.02%) was reported by Tregnago et al., who fabricated PLEDs incorporating in the active layer a phthalimidethiophene host polymer copolymerised with a low-gap D-A-D moiety based on a selenadiaziole. Notably, however, such devices was showed an almost pure NIR EL (88% in the NIR) with maximum at 1000 nm.[28a]

6.3 Donor-acceptor copolymers

Among the different "metal-free" fluorescent materials investigated so far, the best results in the red/NIR region have been obtained by combining electron rich (or donor, D) and electron deficient (or acceptor, A) to obtain "D-A" dyes. Commonly used donor and acceptor moieties are illustrated in **Figure 9.**[28b, 29a-n, 105] Here, we would particularly like to draw the reader's attention to the excellent review on heteroannulated acceptors based on benzothiadiazole by Marder and coworkers, which albeit geared towards PV applications provide a wealth of insight into the electronic structure of these materials.[105b]

One class of low-gap materials that has attracted recent interest in organic electronics is the one based on diketopyrrolopyrrole (DPP) derivatives. DPP derivatives have been already exploited as pigments in several (but not limited to) electronic applications, such as charge generating materials for laser printers, information storage systems, erasable optical memory devices as well as luminescent layers.[23e, 27d, 28e, 28f, 106] In 2002 Beyerlein fabricated OLEDs incorporating a rod-type conjugated copolymer containing a DPP acceptor. These devices exhibited EL peaked at 650 nm (with 15% of the emission in the NIR) and a maximum EQE up to 0.7 % (at 5 V), although these efficiencies significantly drop to 0.4% at an applied voltage of 20 V.[107]

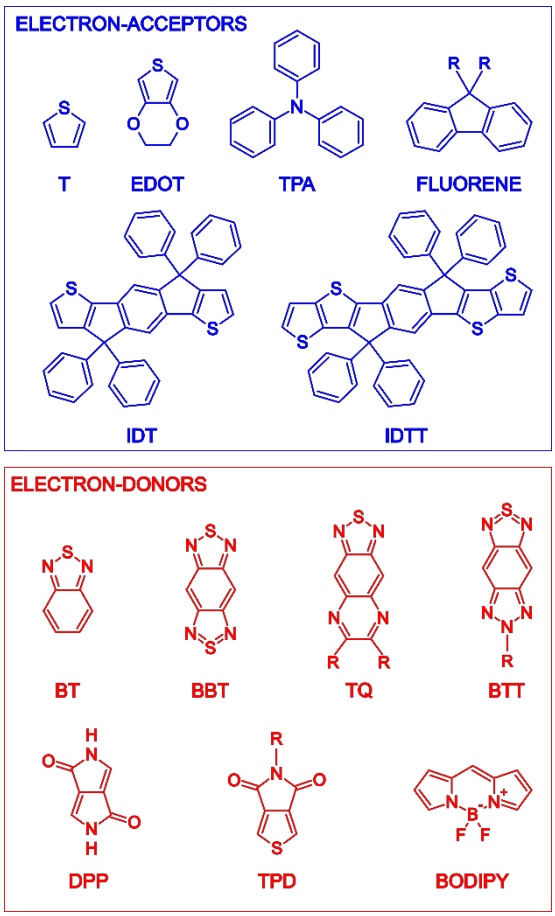

Figure 9. Commonly used electron donor and electron acceptor groups. D: thiophene (T), Ethylenedioxythiophene (EDOT), triphenylamine (TPA), fluorene, indacenodithiophene (IDT), indacenodithienothiophene (IDTT). A: benzothiadiazole (BT), benzobisthiadiazole (BBT), thiadiazoloquinoxaline (TQ), triazolobenzothiadiazole (BTT), diketopyrrolopyrrole (DPP), thienopyrroledione (TPD), boron-dipyrromethene (BODIPY).

Few years later, this issue was addressed (i.e. efficiency tail-off at high driving current densities) by copolymerizing a similar DPP-based D-A-D unit with F8BT, as shown in **Figure 10**, in view of previous results in which F8BT had been used as host for NIR emitting dopants.[52, 108] PLEDs incorporating the DPP-F8BT copolymer exhibited EQEs up to 1% and EL spectrum peaked at 670 nm (NIR emission ~ 40 %) with an output radiance of 1.41 mW/cm^2 and turn-on voltage (V_{ON}) as low as 2.9 V. Interestingly, PLEDs incorporating an interlayer of poly(9,9'-dioctylfluorene-alt-N-(4-butylphenyl)-diphenylamine (TFB) at the interface between the anode

and the active layer [109] showed not only a similar maximum EQE and low V_{ON}, but also a less pronounced roll-off of the efficiency compared to the PLEDs without the TFB interlayer.[110]

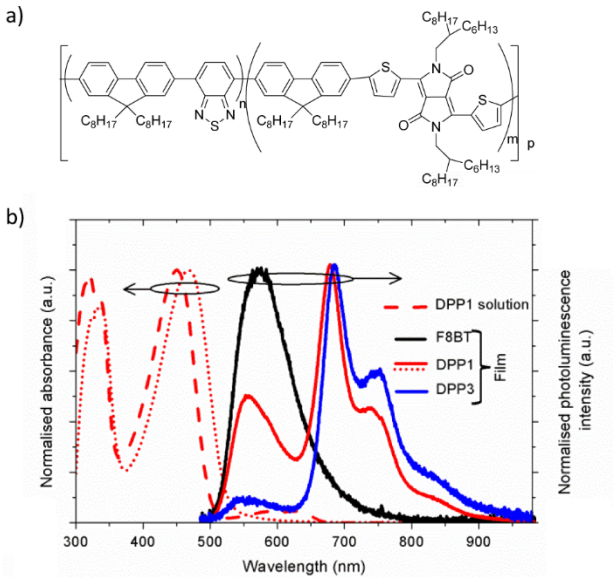

Figure 10. Chemical structures of the emitting polymers used in this study. Note that F8BT has m = 0, whilst DPP1 and DPP3 are random copolymers which differ in the ratio m:n. This ratio is 1:99 for DPP1 and is 3:97 for DPP3. (b) Absorption spectra of DPP1 (red) in solution (dashed) and film (dotted), and photoluminescence spectra (solid lines) of the three synthesized materials in film. Excitation wavelength was 325 nm.[110]

Another example of NIR emitting D-A copolymer was reported by Lombeck et al. in 2016, who fabricated NIR OLEDs exploiting a copolymer based on thiophene−benzothiadiazole−thiophene (TBT) and carbazole (Cbz) alternating repeat units. To increase both solubility and emission efficiency, they modified the chemical structure of copolymer by adding hexyl side chains at the TBT unit. Indeed, from PLEDs based this copolymer, they achieved an EQE of 1% with EL spectrum peaked at 680 nm (NIR emission ~ 40%).[111]

Recently, aiming to shift the EL further into the NIR, we and our collaborators reported a new copolymer series having a BTT derivative as the NIR emitter incorporated in D-A copolymer backbone based on alternating bithiophene and thienopyrroledione (TPD) moieties. PLEDs fabricated with only the neat host polymer already showed a maximum EQEs of 0.49% at 690 nm, with a V_{ON} of only 2.4 V. Notably, however, by incorporating the BTT moieties into the host polymer backbone in a D-A structure, pure NIR emission peaking at ca. 900 nm was measured with and EQE up to 0.15%, in line with the best efficiencies reported in this range from OLEDs with a metal-free active layer.[29m]

6.4 D-A-D and A-D-A oligomers

The same donor and acceptor moieties reviewed in the previous subsection have been also combined to form D-A-D or A-D-A oligomers. For instance, by using D/A building-blocks similar to those used by Lombeck and collaborators,[111] Ledwon reported a class of D-A-D macromolecules based on carbazole as electron-donor and benzothiadiazole as electron-acceptor unit. OLEDs based on such an oligomer exhibited a red-NIR emission peaked at 690 nm with a V_{ON} of 4 V, featuring a remarkable maximum EQE of 3.13%.[112].

Similarly, building on the results from the BTT-doped copolymers reviewed in the previous subsection,[29m] our group also characterised a novel blend featuring a modified BTT emitter (BTT*), engineered to incorporate a central BTT unit in between bithiophenes that act as the donors of a D–A–D structure, and a novel red/NIR emitting polymeric host (PIDT-2TPD), as shown in **Figure 11**, intentionally designed to enhance the charge transport and spectral overlap. Such a host matrix consists of an alternating D–A structure based on indacenodithiophene (IDT) donor and two interconnected TPD acceptors. PLEDs incorporating PIDT-2TPD:BTT* blends exhibited virtually (98%) pure NIR EL peaked at 840 nm with a turn-on voltage of only 1.7 V, EQE up to 1.15%, and an output radiance of ~ 1.5 mW cm^{-2}.

Interestingly, such devices can operate up to 200 mA cm^{-2} while maintaining the EQE above 0.5%.[29n]

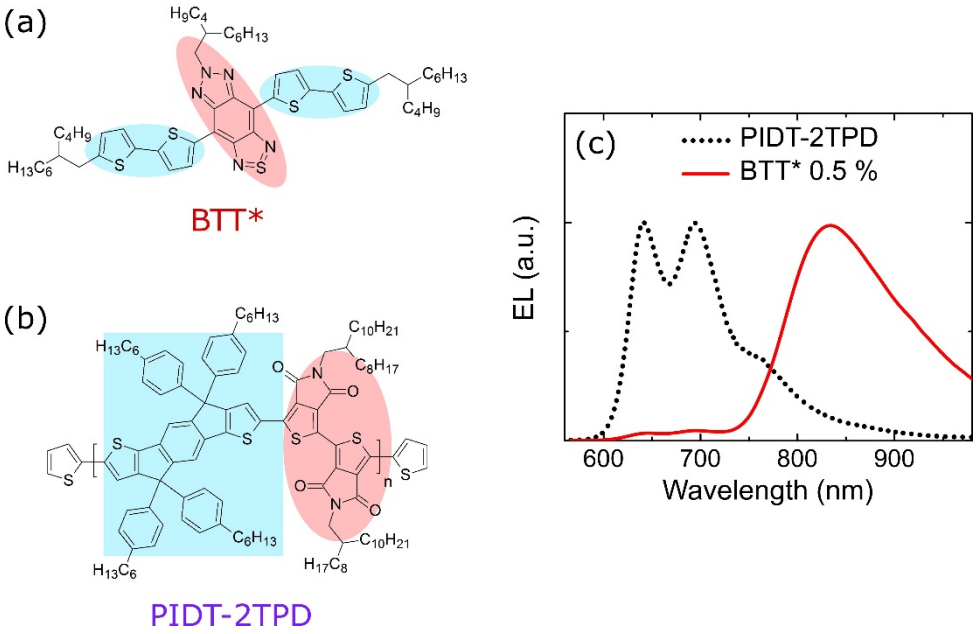

Figure 11. (a,b) Molecular structures of the BTT* NIR dye and PIDT-2TPD host polymers. Pale blue and red shadings highlight the electron donor and acceptor units, respectively. (c) EL spectra of PLEDs incorporating PIDT-2TPD, and blend with 0.5 wt% of BTT*.[6a]

Another family of D-A-D NIR emitting oligomers was reported in 2011 by Ellinger et al..[100] Such dyes consisted of electron-withdrawing benzothiadiazole (BT) derivatives and electron-releasing groups such as such thiophene and 3,4-ethylenedioxythiophene (EDOT). Interestingly, they achieved EQEs of ca. 0.5% with EL peak at 725 nm by blending an EDOT-BT-EDOT based oligomer in a MEH-PPV matrix.[100]

More recently, Yao et al. reported OLEDs with EQEs > 1% based on a series of NIR emitting oligomers, some of which presenting an A-D-A molecular structure.[29j] In this regard, it is important to highlight that, whereas the properties of dyes of the D-A-D type have been studied extensively, different alternation patterns of the D and A moieties and in particular, A-

D-A dyes have rarely been explored in the literature. The main challenges are the synthetic difficulties associated to the monofunctionalization of the A building block. Furthermore, the D-A-D and A-D-A systems presented by Yao benefit also from a favourable conformational arrangement of the constituting units, which controls the orbital mixing and leads to the formation of a hybrid localised/charge-transfer (CT) excited state. It was proposed that the localised nature of these states brings about a high radiative rate, whereas the weakly bound CT nature leads to the formation of a high fraction (> 25%) of singlet excitons.[29j, 29k]

Another example of A-D-A oligomer emitting in the NIR leveraged a breakthrough in the synthesis of α,β-unfunctionalised 4,4-difluoro-4-bora-3a,4a-diaza-s-indacene (BODIPY, Figure 9). Such an A-D-A oligomer is formed by two BODIPY moieties connected through their meso-positions to an α,ω-oligothiophene core, as shown in **Figure 12**. The NIR emission from this dye is promoted by the delocalisation of the BODIPY low-lying LUMO over the oligothienyl moieties, as confirmed by density functional theory (DFT). In addition, as extrapolated from cyclovoltammetry measurements and DFT data, the intramolecular energy structure of such oligomer should favour a "hole funnelling" effect towards the central part of the molecule in the presence of a substantially homogeneous distribution of electrons on a relatively low-lying LUMO, that could for example be populated effectively from a host polymer (such as F8BT) in a guest-host emitting layer. The added potential bonus of this structure is that the resulting excitons should therefore localize on the central part of the molecule, and thus be less exposed to quenching by neighbouring moieties or contaminants. PLEDs incorporating NIRBDTE in blend with F8BT exhibited emission at 720 nm with EQEs up to 1.1%. This result demonstrates the potential of the A-D-A motif, that is still a "scarcely-studied" class of red/NIR emitters.[29l]

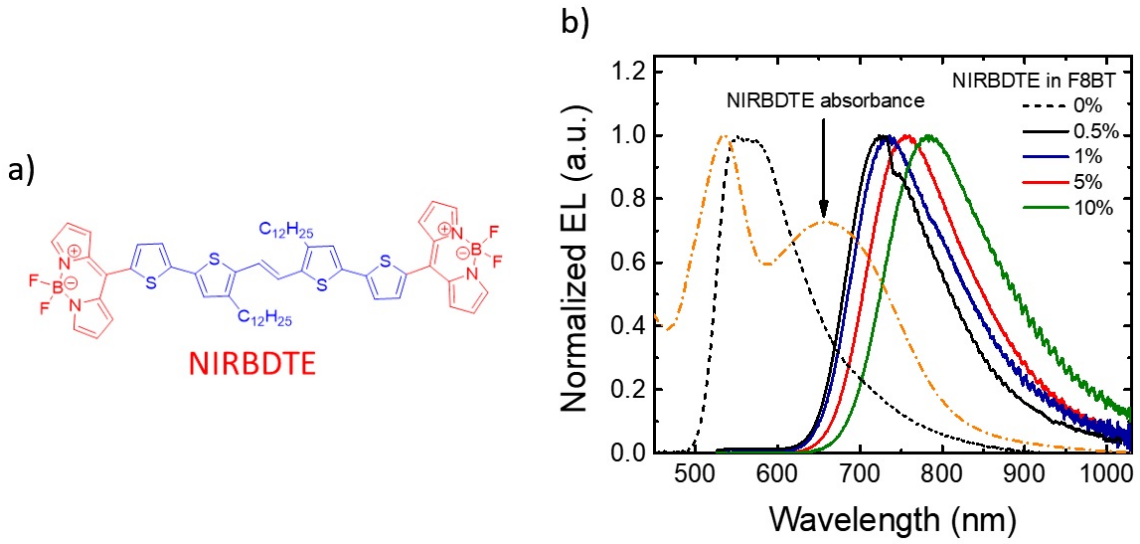

Figure 12. a) Chemical structure of F8BT and NIRBDTE. b) EL spectra of PLEDs incorporating different NIRBDTE concentration in the host F8BT.[34e]

Even in the presence of significant progress, as highlighted above, the achievement of NIR fluorescence exclusively above 1000 nm is still an open-challenge. One of the rare successful attempts has been reported by Chen et al. in 2004, exploiting an alternating conjugated polymer based on fluorene units and low-band gap D-A-D units. The D-A-D segment includes two electron-donating thiophene rings combined with a thiadiazoloquinoxaline (TQ) unit as electron acceptor units, featuring a band gap of 1.27 eV. The electro- and photoluminescence spectra were peaked at 970 nm and approximately 1 μm, respectively. OLEDs incorporating this copolymer exhibited a maximum EQE of 0.05%.[103]

Qian et al. also reported in 2009 a series of NIR organic D-A-D chromophores based on a benzobisthiadiazole (BBT) derivative as acceptor and different donor groups, exhibiting both PL and EL above 1000 nm.[11] In particular, the D-A-D molecule featuring triphenylamine (TPA) as donor group exhibited a maximum EL EQE of 0.28% and EL peaked at 1008 nm when incorporated as emitting layer in a non-doped OLED.[11]

6.5 NIR fluorophores featuring AIE

As discussed in Section 2.3, largely conjugated NIR fluorophores suffer from strong aggregation-caused emission quenching. However, as observed for some TADF emitters,[39b] some D-A-D NIR fluorophores can exhibit AIE. In 2012, Du et al. reported a new family of D-A-D NIR emitting fluorophores containing rigid nonplanar conjugated tetraphenylethene (TPE) moieties with electron-deficient BBT and TQ (Figure 9) as acceptors. Such compounds exhibited good AIE properties, as a result of the twisted TPE units, which limit the intramolecular rotation and reduce the π–π stacking. OLEDs incorporating the TPE-TQ-TPE D-A-D compound in the active layer exhibited a maximum EQE of 0.89% with an emission peaked at 706 nm.[39a]

Recently, by leveraging the same TPE AIE building block, we and our collaborators reported a new class of emitters based on a BODIPY derivative, functionalized at different positions with TPE. PL of the functionalised BODIPY moieties shifts from the green to the NIR spectral range as a result of the different TPE position in the chemical structure. In particular, 2,6,8-tri-TPE-substituted BODIPY dyes exhibited PL efficiency up to 39% in the solid state. Furthermore, when a small amount (1%) of these tri-TPE-substituted emitters was diluted in a F8BT matrix, the resulting blend exhibited a ϕ_{FL} up to 100%, with PL peaked at 720 nm. Notably, by incorporating such blends in the active layer of solution-processed PLEDs, we obtained EL in the range 650–700 nm with up to 1.8% EQE and ~ 2 mW/cm^2 radiance.[39c]

6.6 Other classes of NIR fluorophores

With the aim of shifting the emission of NIR OLEDs to wavelengths beyond 800 nm, recently Graf et al. proposed single-walled carbon nanotubes (SWCNTs) as an alternative solution to organic and organometallic chromophores.[104] By incorporating SWCNTs in a multilayer-stacked OLED architecture, they obtained EL featuring two narrow bands peaking

at wavelengths between 1000 and 1200 nm, corresponding to an excitonic and a trionic transition, respectively. Although the maximum EQE of such devices was limited to 0.014%, the authors suggest that SWCNT OLEDs could offer several advantages with respect to other classes of NIR emitting dyes, mainly related to their photo- and thermal-stability. Furthermore, by varying the diameter and the chirality of the SWCNTs, or through their chemical modification, the emission of SWCNT OLEDs could be tuned across the entire NIR range.

Squaraine derivatives provide another class of promising fluorophores emitting in the NIR. Thanks to their strong and narrow emission bands in the red/NIR region, squaraine dyes have been widely used for biosensing applications[113] and organic photovoltaics, either as sensitizers (e.g. in dye-sensitized solar cells, DSSCs) or as electron-donors in bulk-heterojunctions.[114] So far, the most efficient OLEDs integrating a squaraine dye as fluorophore have been reported by Stender et al. in 2013, who obtained an EL EQE of 0.65% (EL peaked at 550 nm and 730 nm) from OLEDs incorporating a bromoindolenine squaraine dopant in blend with the highly fluorescent PPV derivative.[101].

7. Future Perspectives

7.1 Existing and potential application areas

There is little doubt that development of NIR-OLEDs is being driven more as a "technology push" rather than as a "market pull", but it is still true that the list of potential applications for NIR-emitting LEDs in general (organics included) keeps growing, and now spans from security, to bio-sensing (e.g. blood oxymetry), photodynamic therapy (both thermally-mediated therapy, e.g. with nanoparticle-mediated absorption, and via drug-activation), and short-range (last-meter or so) through space communications (TSCs) systems.

Security applications include personal identification, as in Apple's patent for a device in which the OLED display also incorporate NIR emitters and detectors for fingerprint detection, [[115]] for example, but could extend in the future to capillary vein mapping (fingers, palm, or eyes) to reduce identification errors and subsequent fraud.[18-19]

As mentioned above the semitransparency of biological tissue to radiation between 700 and 1000 nm appears to be a relatively fortunate coincidence for both those applications above and more generally for biosensing (and phototherapy), although this has not yet been exploited very much and only few examples, mainly related to the measurement of blood oxygenation (oxymetry), have been produced so far.[14]

TSCs are being explored mainly in connection with visible emitters, and thus more often termed "visible light communications (VLCs)" systems, but it is nevertheless obvious that these would significantly benefit from the additional bandwidth that can be brought about by the integration of additional NIR emitters. In addition, a potential significant advantage would be the possibility to integrate TSCs systems within OLEDs lighting solutions, in turn predicted to generate a market of up to USD 2.5 billions by 2027 according to IDTECHEX[116]. In perspective, another intriguing area of application for NIR OLEDs is that of optogenetics, in very general terms the use of light for controlling cells behaviour *in vivo* and with special emphasis on neurons.[117] Most optogenetics so far has been limited to the use of visible (in fact blue) sources, but NIR radiation can bring advantages both in terms of longer penetration depths and lower damage to the living tissues nearby, and can be pursued either via up-conversion schemes in combination with existing visible fluorescent proteins and receptors, or via molecular engineering of the so-called "opsins" so as enable truly NIR optogenetics, which should also minimise tissue damage and cell phototoxicity effects compared to the use of shorter wavelengths.

Similar considerations, but with a significantly augmented impact scope, apply to the possibility of using NIR-OLEDs in the contest of gene editing with the CRISPR/CAS-9 (Clustered Regularly Interspaced Short Palindromic Repeats / CRISPR Associated protein 9) methods,[118] i.e. for stimulation of so-called light-activated CRISPR/CAS9 effectors (LACE), so far mostly confined to the use of blue-light,[119]again with shortcomings in terms of penetration depth and phototoxicity.

7.2 Materials and devices

Progress in all the key performance parameters of NIR-OLEDs, and especially efficiency, radiance and operative lifetime are required for commercial exploitation, because for essentially all the fields above there clearly is strong competition from alternative technologies, mainly based on inorganic emitters. Toxicity concerns aside, some of these, such as quantum dots (PbS, or PbSe for example),[120] also promise similar solution-processing advantages compared to organic semiconductors, but come with significantly higher efficiency. Of course, it can be argued that phosphorescent OLEDs also offer high efficiency, albeit at shorter wavelengths compared to PbS, while needing only a fraction of the heavy metals.

While both material parameters and device engineering are important for device performance, most progress has come from materials development over the past years, with the overall device sandwich structure remaining essentially unchanged and comprising an active layer between two electrodes. It is therefore reasonable to expect this trend will continue.

Device development has focused mostly on electrodes work function engineering (for which there is limited need with NIR emitters, as discussed earlier), and insertion of charge injection/blocking (or transport) layers as well as exciton blocking layers to avoid excitons being quenched at electrodes (especially for phosphorescent devices).

Interestingly, organic light-emitting transistors (OLETs) provide a wholly different device architecture that has shown intriguing performance figures for visible emitters[121] and that offers specific opportunities for NIR emitters because of the already mentioned modest need of electrodes work function engineering, which allows fabrication of OLETs with the same electrodes material for injection of both electrons and holes.[104, 122] This is potentially a big simplification, although it remains to be assessed if the residual energy barriers are compatible with commercial development of NIR-OLETs. Any residual barrier is in fact bound to increase the (already) relatively high source-drain voltage typically needed for OLETs operation, in turn brought about by the relatively long channel lengths (few micrometres) afforded by reasonably-cheap conventional patterning of the electrodes. Additional concerns for the OLET architecture are about the active area of the devices being reduced by the electrodes area, but this can possibly become acceptable if suitably managed, and especially if the reduced active area is offset by high radiance and efficiency from such active areas.

Examining next the materials perspectives we note that significant progress has already been achieved by implementation of several chemical design strategies, as reviewed above, and with some remarkable results in terms of efficiency for all the three main classes of NIR-OLEDs: phosphorescent, triplet-leveraging fluorescent (TADF - TTA), and purely fluorescent, possibly hinting that the progress needed for any commercialisation might by now be more related to device lifetime and durability than to EQEs.

A closer look at **Table 1** also shows, however, that some of the more impressive EQEs (in some cases even close to the theoretical limit such as for phosphorescent devices)[6b] are for materials with emission peaks very near the 700 nm blue end of the NIR range we have chosen here (Table 1-3). Pushing for higher efficiency at longer wavelength would thus appear to be

another obvious next step (in addition to increasing lifetime) to enable a wider range of potential applications, and hopefully a "killer application" as well, which is what is still missing.

On the basis of the challenges outlined in Section 2 it follows that success at extending the emission range further into the NIR will require careful management of both aggregation and of the radiationless deactivation of the excited states predicted by the so-called "energy-gap law". However, although there have been a few reports of experimental trends in qualitative agreement with such a law for materials series with very similar molecular structures, it is important to note that judicious control of aggregation has in some cases raised the materials luminescence efficiency beyond expectations.[123] While such results raise interesting fundamental questions on the importance of the interplay between aggregation and energy-gap effects, as well as on the generality of the applicability of the E_G law, they also leave ample scope for an optimistic outcome of a material development programme through control of aggregation in the first place, e.g. via suppression of detrimental (H-type) aggregation, or possibly via pursuit of aggregation-induced emission of which relatively few examples have been reported in the NIR.

Coming back to the prospects of a "killer application", this could for example be generated within the territory of organic bioelectronics,[124] that is commanding increasing attention from both academic and industrial communities. In this regard and as noted already in this review, TADF materials and those leveraging AIE have an inherent "low-toxicity" advantage, and appear thus to be the way forward. Although significant additional experimentation might be needed to obtain regulatory approval for *in vivo* applications, it is reasonable to expect that this would be substantially easier than for inorganic quantum dots and phosphorescent materials.

As expected, competition by inorganic NIR (and visible) emitters is particularly strong for application to TSCs, primarily because of the better performance of inorganics in terms of power, bandwidth and durability, but also because of less stringent requirement on the non-toxicity of the materials for such applications. Among organic ones, fluorescent NIR-OLEDs only leveraging singlet emission (i.e. excluding those leveraging triplets harvesting via TADF or TTA, but including those leveraging aggregation-induced emission), are expected to offer better prospects for TSCs compared to triplet-leveraging ones, given that the ultimate bandwidth is limited by the luminescence lifetime, of the order of few ns for the first class (i.e. harvesting singlets only) compared to microseconds or so for triplets leveraging ones (via TADF, TTA and phosphorescence). Interestingly these are also the materials for which there likely are larger margins for potential improvement (e.g. the current highest EQE for 720 nm exceeds 1%) for example via judicious exploitation of AIE.

Looking further into the future, some recent results suggest that the above mentioned classes of organic NIR emitters, relying either on singlet or triplet harvesting, will also have to compete with chromophores containing neutral π-radical moieties, which exploit doublet excitons to reach up to 100% IQE.[125] Obolda et al. have shown in 2016 that OLEDs incorporating a neutral π-radical as emitter can exhibit EL peaked at 700 nm with EQE reaching up to 4.3%.[125c] The main advantage of using such materials with respect to the singlet and triplet leveraging ones is that they combine both high IQEs and relatively short (< 100 ns) exciton recombination dynamics, with the latter arising from the spin-allowed transition from the doublet excited state to the doublet ground state.[125]

In concluding, we very much hope this necessarily limited account of recent research on NIR-OLEDs will instigate further interest in this area, both at academic and industrial level, thereby acting as a catalyst of further basic understanding of the processes characterising

radiative emission in this spectral range, and, most importantly, underpinning further device development capable of significant societal impact.

Last but not least, we can only offer our sincere apologies for any omission of relevant published work due to the non-exhaustive nature of this review.

8. Acknowledgments

AZ and AM contributed equally to this work. The authors gratefully acknowledge funding by the European Community's Seventh Framework Programme (FP7/2007-2013) ITN MSCA action under Grant Agreement No. 607585 (OSNIRO) and by EPSRC (grant EP/P006280/1). FC is a Royal Society Wolfson Merit Award holder.

[1] a) C. W. Tang, S. A. VanSlyke, *Appl. Phys. Lett.* **1987**, *51*, 913; b) J. H. Burroughes, D. D. C. Bradley, A. R. Brown, R. N. Marks, K. Mackay, R. H. Friend, P. L. Burns, A. B. Holmes, *Nature* **1990**, *347*, 539.

[2] a) D. T. McQuade, J. Kim, T. M. Swager, *Journal of American Chemical Society* **2000**, *122*, 5885; b) F. Cacialli, J. S. Wilson, J. J. Michels, C. Daniel, C. Silva, R. H. Friend, N. Severin, P. Samorì, J. P. Rabe, M. J. O'Connell, P. N. Taylor, H. L. Anderson, *Nature materials* **2002**, *1*, 160; c) Y. N. Hong, J. W. Y. Lam, B. Z. Tang, *Chemical Society Reviews* **2011**, *40*, 5361.

[3] M. A. Baldo, D. F. Obrien, Y. You, A. Shoustikov, S. Sibley, M. E. Thompson, S. R. Forrest, *Nature* **1998**, *395*, 151.

[4] T. M. Brown, J. S. Kim, R. H. Friend, F. Cacialli, R. Daik, W. J. Feast, *Applied Physics Letters* **1999**, *75*, 1679.

[5] a) M. Berggren, M. Granstrom, O. Inganas, M. Andersson, *Advanced Materials* **1995**, *7*, 900; b) T. C. Chao, Y. T. Lin, C. Y. Yang, T. S. Hung, H. C. Chou, C. C. Wu, K. T. Wong, *Advanced Materials* **2005**, *17*, 992; c) T. Z. Yu, W. M. Su, W. L. Li, R. N. Hua, B. Chu, B. Li, *Solid-State Electronics* **2007**, *51*, 894; d) S. Kervyn, O. Fenwick, F. Di Stasio, Y. S. Shin, J. Wouters, G. Accorsi, S. Osella, D. Beljonne, F. Cacialli, D. Bonifazi, *Chem.-Eur. J.* **2013**, *19*, 7771; e) Y. X. Yang, P. Cohn, S. H. Eom, K. A. Abboud, R. K. Castellano, J. G. Xue, *Journal of Materials Chemistry C* **2013**, *1*, 2867; f) S. F. Varol, S. Sayin, S. Eymur, Z. Merdan, D. Unal, *Organic Electronics* **2016**, *31*, 25.

[6] a) A. Minotto, P. Murto, Z. Genene, A. Zampetti, G. Carnicella, W. Mammo, M. R. Andersson, E. Wang, F. Cacialli, *Advanced Materials* **2018**, *30*, 1706584; b) K. Tuong

Ly, R.-W. Chen-Cheng, H.-W. Lin, Y.-J. Shiau, S.-H. Liu, P.-T. Chou, C.-S. Tsao, Y.-C. Huang, Y. Chi, *Nature Photonics* **2017**, *11*, 63; c) D. H. Kim, A. D'Aléo, X. K. Chen, A. D. S. Sandanayaka, D. Yao, L. Zhao, T. Komino, E. Zaborova, G. Canard, Y. Tsuchiya, E. Choi, J. W. Wu, F. Fages, J. L. Brédas, J. C. Ribierre, C. Adachi, *Nature Photonics* **2018**, *12*, 98.

[7] A. M. Smith, M. C. Mancini, S. Nie, *Nature Nanotechnology* **2009**, *4*, 710.

[8] F. C. Spano, C. Silva, *Annual review of physical chemistry* **2014**, *65*, 477.

[9] R. Englman, J. Jortner, *Molecular Physics* **1970**, *18*, 145.

[10] a) S. T. Le, T. Kanesan, F. Bausi, P. a. Haigh, S. Rajbhandari, Z. Ghassemlooy, I. Papakonstantinou, W. O. Popoola, A. Burton, H. Le Minh, F. Cacialli, A. D. Ellis, *Optics Letters* **2014**, *39*, 3876; b) P. A. Haigh, F. Bausi, Z. Ghassemlooy, I. Papakonstantinou, H. Le Minh, C. Flechon, F. Cacialli, *Opt Express* **2014**, *22*, 2830.

[11] G. Qian, Z. Zhong, M. Luo, D. Yu, Z. Zhang, Z. Y. Wang, D. Ma, *Advanced Materials* **2009**, *21*, 111.

[12] a) K. H. Hendriks, W. Li, M. M. Wienk, R. A. Janssen, *Journal of the American Chemical Society* **2014**, *136*, 12130; b) C. Liu, K. Wang, X. Gong, A. J. Heeger, *Chemical Society Reviews* **2016**, *45*, 4825.

[13] L. Meng, Y. Zhang, X. Wan, C. Li, X. Zhang, Y. Wang, X. Ke, Z. Xiao, L. Ding, R. Xia, H.-L. Yip, Y. Cao, Y. Chen, *Science* **2018**, *361*, 1094.

[14] a) C. M. Lochner, Y. Khan, A. Pierre, A. C. Arias, *Nature communications* **2014**, *5*, 5745; b) Y. Khan, A. E. Ostfeld, C. M. Lochner, A. Pierre, A. C. Arias, *Advanced Materials* **2016**, *28*, 4373.

[15] L. Maggini, I. Cabrera, A. Ruiz-Carretero, E. A. Prasetyanto, E. Robinet, L. De Cola, *Nanoscale* **2016**, *8*, 7240.

[16] C. Shirata, J. Kaneko, Y. Inagaki, T. Kokudo, M. Sato, S. Kiritani, N. Akamatsu, J. Arita, Y. Sakamoto, K. Hasegawa, N. Kokudo, *Sci Rep* **2017**, *7*, 13958.

[17] X. B. Han, H. X. Li, Y. Q. Jiang, H. Wang, X. S. Li, J. Y. Kou, Y. H. Zheng, Z. N. Liu, H. Li, J. Li, D. Dou, Y. Wang, Y. Tian, L. M. Yang, *Cell Death and Disease* **2017**, *8*, e2864.

[18] a) M. Kono, H. Ueki, S.-i. Umemura, *Appl. Opt.* **2002**, *41*, 7429; b) E. C. Lee, H. Jung, D. Kim, *Sensors* **2011**, *11*, 2319.

[19] M. A. M. Abdullah, J. A. Chambers, W. L. Woo, S. S. Dlay, *Proceedings - 3rd IAPR Asian Conference on Pattern Recognition, ACPR 2015* **2016**, DOI: 10.1109/ACPR.2015.7486616816.

[20] V. C. Bender, T. B. Marchesan, J. M. Alonso, *IEEE Industrial Electronics Magazine* **2015**, *9*, 6.

[21] G. Crawford, *Flexible flat panel displays*, John Wiley & Sons, **2005**.

[22] J. Park, D. Shin, S. Park, *Semiconductor Science and Technology* **2011**, *26*, 034002.

[23] a) E. J. Meijer, D. M. De Leeuw, S. Setayesh, E. Van Veenendaal, B. H. Huisman, P. W. M. Blom, J. C. Hummelen, U. Scherf, T. M. Klapwijk, *Nature materials* **2003**, *2*, 678; b) T. D. Anthopoulos, S. Setayesh, E. Smits, M. Cölle, E. Cantatore, B. De Boer, P. W. M. Blom, D. M. De Leeuw, *Advanced Materials* **2006**, *18*, 1900; c) L. Bürgi, M. Turbiez, R. Pfeiffer, F. Bienewald, H. J. r. Kirner, C. Winnewisser, *Advanced Materials* **2008**, *20*, 2217; d) J. D. Yuen, R. Kumar, D. Zakhidov, J. Seifter, B. Lim, A. J. Heeger, F. Wudl, *Advanced Materials* **2011**, *23*, 3780; e) C. B. Nielsen, M. Turbiez, I. McCulloch, *Advanced Materials* **2013**, *25*, 1859; f) T. Jiang, Z. Xue, M. Ford, J. Shaw, X. Cao, Y. Tao, Y. Hu, W. Huang, *RSC Advances* **2016**, *6*, 78720; g) K. Kawabata, M.

Saito, I. Osaka, K. Takimiya, *Journal of the American Chemical Society* **2016**, *138*, 7725; h) J. Zaumseil, H. Sirringhaus, *Chemical reviews* **2007**, *107*, 1296.

[24] a) T. M. Brown, F. Cacialli, *Journal of Polymer Science Part B: Polymer Physics* **2003**, *41*, 2649; b) P. K. H. Ho, J. S. Kim, J. H. Burroughes, H. Becker, S. F. Y. Li, T. M. Brown, F. Cacialli, R. H. Friend, *Nature* **2000**, *404*, 481.

[25] a) J. L. Brédas, *The Journal of chemical physics* **1985**, *82*, 3808; b) J. Roncali, *Macromolecular Rapid Communications* **2007**, *28*, 1761; c) R. L. Gieseking, C. Risko, J. L. Bredas, *J Phys Chem Lett* **2015**, *6*, 2158.

[26] J. Huber, K. Mullen, J. Salbeck, H. Schenk, U. Scherf, T. Stehlin, R. Stern, *Acta Polym.* **1994**, *45*, 244.

[27] a) J. R. Sommer, A. H. Shelton, A. Parthasarathy, I. Ghiviriga, J. R. Reynolds, K. S. Schanze, *Chemistry of Materials* **2011**, *23*, 5296; b) H. Zhong, Z. Li, F. Deledalle, E. C. Fregoso, M. Shahid, Z. Fei, C. B. Nielsen, N. Yaacobi-Gross, S. Rossbauer, T. D. Anthopoulos, J. R. Durrant, M. Heeney, *Journal of the American Chemical Society* **2013**, *135*, 2040; c) H. Zhong, Y. Han, J. Shaw, T. D. Anthopoulos, M. Heeney, *Macromolecules* **2015**, *48*, 5605; d) M. Grzybowski, V. Hugues, M. Blanchard-Desce, D. T. Gryko, *Chemistry - A European Journal* **2014**, *20*, 12493; e) G. M. Paternò, Q. Chen, X. Y. Wang, J. Liu, S. G. Motti, A. Petrozza, X. Feng, G. Lanzani, K. Müllen, A. Narita, F. Scotognella, *Angewandte Chemie - International Edition* **2017**, *56*, 6753.

[28] a) G. Tregnago, T. T. Steckler, O. Fenwick, M. R. Andersson, F. Cacialli, *J. Mater. Chem. C* **2015**, *3*, 2792; b) A. J. Kronemeijer, E. Gili, M. Shahid, J. Rivnay, A. Salleo, M. Heeney, H. Sirringhaus, *Advanced Materials* **2012**, *24*, 1558; c) R. Q. Yang, R. Y. Tian, Q. Hou, W. Yang, Y. Cao, *Macromolecules* **2008**, *41*, 8951; d) W. C. Tsoi, D. T. James, E. B. Domingo, J. S. Kim, M. Al-Hashimi, C. E. Murphy, N. Stingelin, M. Heeney, J. S. Kim, *ACS nano* **2012**, *6*, 9646; e) M. Shahid, T. McCarthy-Ward, J. Labram, S. Rossbauer, E. B. Domingo, S. E. Watkins, N. Stingelin, T. D. Anthopoulos, M. Heeney, *Chemical Science* **2012**, *3*, 181; f) M. Shahid, R. S. Ashraf, Z. G. Huang, A. J. Kronemeijer, T. McCarthy-Ward, I. McCulloch, J. R. Durrant, H. Sirringhaus, M. Heeney, *Journal of Materials Chemistry* **2012**, *22*, 12817; g) D. Patra, J. Lee, S. Dey, J. Lee, A. J. Kalin, A. Putta, Z. Fei, T. McCarthy-Ward, H. S. Bazzi, L. Fang, M. Heeney, M. H. Yoon, M. Al-Hashimi, *Macromolecules* **2018**, *51*, 6076; h) A. J. Kronemeijer, E. Gili, M. Shahid, J. Rivnay, A. Salleo, M. Heeney, H. Sirringhaus, *Advanced Materials* **2012**, *24*, 1558; i) M. Heeney, W. Zhang, D. J. Crouch, M. L. Chabinyc, S. Gordeyev, R. Hamilton, S. J. Higgins, I. McCulloch, P. J. Skabara, D. Sparrowe, S. Tierney, *Chemical Communications* **2007**, DOI: 10.1039/b712398a5061; j) Z. P. Fei, Y. Han, E. Gann, T. Hodsden, A. S. R. Chesman, C. R. McNeill, T. D. Anthopoulos, M. Heeney, *Journal of the American Chemical Society* **2017**, *139*, 8552; k) D. J. Crouch, P. J. Skabara, J. E. Lohr, J. J. W. McDouall, M. Heeney, I. McCulloch, D. Sparrowe, M. Shkunov, S. J. Coles, P. N. Horton, M. B. Hursthouse, *Chemistry of Materials* **2005**, *17*, 6567; l) D. J. Crouch, P. J. Skabara, M. Heeney, I. McCulloch, D. Sparrowe, S. J. Coles, M. B. Hursthouse, *Macromolecular Rapid Communications* **2008**, *29*, 1839; m) Z. Y. Chen, H. Lemke, S. Albert-Seifried, M. Caironi, M. M. Nielsen, M. Heeney, W. M. Zhang, I. McCulloch, H. Sirringhaus, *Advanced Materials* **2010**, *22*, 2371; n) A. M. Ballantyne, L. C. Chen, J. Nelson, D. D. C. Bradley, Y. Astuti, A. Maurano, C. G. Shuttle, J. R. Durrant, M. Heeney, W. Duffy, I. McCulloch, *Advanced Materials* **2007**, *19*, 4544; o) M. Al-Hashimi, Y. Han, J. Smith, H. S. Bazzi, S. Y. A. Alqaradawi, S. E. Watkins, T. D. Anthopoulos, M. Heeney, *Chemical Science* **2016**, *7*, 1093; p) R. Q. Yang, R. Y. Tian, J. G. Yan, Y. Zhang, J. Yang, Q. Hou, W. Yang, C. Zhang, Y. Cao,

Macromolecules **2005**, *38*, 244; q) G. L. Gibson, T. M. McCormick, D. S. Seferos, *Abstr. Pap. Am. Chem. Soc.* **2012**, *243*, 1.

[29] a) G. Qian, Z. Y. Wang, *Chemistry–An Asian Journal* **2010**, *5*, 1006; b) G. W. Van Pruissen, F. Gholamrezaie, M. M. Wienk, R. A. Janssen, *Journal of Materials Chemistry* **2012**, *22*, 20387; c) K. H. Hendriks, W. W. Li, M. M. Wienk, R. A. J. Janssen, *Journal of the American Chemical Society* **2014**, *136*, 12130; d) R. S. Ashraf, I. Meager, M. Nikolka, M. Kirkus, M. Planells, B. C. Schroeder, S. Holliday, M. Hurhangee, C. B. Nielsen, H. Sirringhaus, *Journal of the American Chemical Society* **2015**, *137*, 1314; e) J. D. Yuen, R. Kumar, D. Zakhidov, J. Seifter, B. Lim, A. J. Heeger, F. Wudl, *Advanced Materials* **2011**, *23*, 3780; f) T. L. D. Tam, T. Salim, H. Li, F. Zhou, S. G. Mhaisalkar, H. Su, Y. M. Lam, A. C. Grimsdale, *Journal of Materials Chemistry* **2012**, *22*, 18528; g) T. Dallos, D. Beckmann, G. Brunklaus, M. Baumgarten, *Journal of the American Chemical Society* **2011**, *133*, 13898; h) R. S. Ashraf, A. J. Kronemeijer, D. I. James, H. Sirringhaus, I. McCulloch, *Chemical Communications* **2012**, *48*, 3939; i) Z. Fei, X. Gao, J. Smith, P. Pattanasattayavong, E. Buchaca Domingo, N. Stingelin, S. E. Watkins, T. D. Anthopoulos, R. J. Kline, M. Heeney, *Chemistry of Materials* **2012**, *25*, 59; j) L. Yao, S. Zhang, R. Wang, W. Li, F. Shen, B. Yang, Y. Ma, *Angewandte Chemie International Edition* **2014**, *53*, 2119; k) X. Han, Q. Bai, L. Yao, H. Liu, Y. Gao, J. Li, L. Liu, Y. Liu, X. Li, P. Lu, *Advanced Functional Materials* **2015**, *25*, 7521; l) A. Zampetti, A. Minotto, B. M. Squeo, V. G. Gregoriou, S. Allard, U. Scherf, C. L. Chochos, F. Cacialli, *Scientific Reports* **2017**, *7*; m) P. Murto, A. Minotto, A. Zampetti, X. F. Xu, M. R. Andersson, F. Cacialli, E. G. Wang, *Advanced Optical Materials* **2016**, *4*, 2068; n) A. Minotto, P. Murto, Z. Genene, A. Zampetti, G. Carnicella, W. Mammo, M. R. Andersson, E. G. Wang, F. Cacialli, *Advanced Materials* **2018**, *30*; o) L. Beverina, G. A. Pagani, *Accounts of chemical research* **2014**, *47*, 319.

[30] G. Tregnago, C. Fléchon, S. Choudhary, C. Gozalvez, a. Mateo-Alonso, F. Cacialli, *Applied Physics Letters* **2014**, *105*, 143304.

[31] H. Xiang, J. Cheng, X. Ma, X. Zhou, J. J. Chruma, *Chemical Society reviews* **2013**, *42*, 6128.

[32] H. Bässler, *Macromol. Symp.* **1996**, *104*, 269.

[33] a) S. Brovelli, F. Meinardi, G. Winroth, O. Fenwick, G. Sforazzini, M. J. Frampton, L. Zalewski, J. a. Levitt, F. Marinello, P. Schiavuta, K. Suhling, H. L. Anderson, F. Cacialli, *Advanced Functional Materials* **2010**, *20*, 272; b) S. Brovelli, G. Sforazzini, M. Serri, G. Winroth, K. Suzuki, F. Meinardi, H. L. Anderson, F. Cacialli, *Advanced Functional Materials* **2012**, *22*, 4284.

[34] a) J. Morgado, F. Cacialli, R. Iqbal, S. Moratti, A. Holmes, G. Yahioglu, L. Milgrom, R. Friend, *Journal of Materials Chemistry* **2001**, *11*, 278; b) F. Cacialli, M. Stoneham, *J. Phys.-Condes. Matter* **2002**, *14*, V9; c) K. R. Graham, Y. Yang, J. R. Sommer, A. H. Shelton, K. S. Schanze, J. Xue, J. R. Reynolds, *Chemistry of Materials* **2011**, *23*, 5305; d) O. Fenwick, J. K. Sprafke, J. Binas, D. V. Kondratuk, F. Di Stasio, H. L. Anderson, F. Cacialli, *Nano letters* **2011**, *11*, 2451; e) A. Zampetti, A. Minotto, B. M. Squeo, V. G. Gregoriou, S. Allard, U. Scherf, C. L. Chochos, F. Cacialli, *Scientific Reports* **2017**, *7*, 1611.

[35] a) J. Morgado, F. Cacialli, R. Friend, R. Iqbal, G. Yahioglu, L. Milgrom, S. Moratti, A. Holmes, *Chemical Physics Letters* **2000**, *325*, 552; b) T. T. Steckler, M. J. Lee, Z. Chen, O. Fenwick, M. R. Andersson, F. Cacialli, H. Sirringhaus, *Journal of Materials Chemistry C* **2014**, *2*, 5133; c) D. M. E. Freeman, A. Minotto, W. Duffy, K. J. Fallon, I. McCulloch, F. Cacialli, H. Bronstein, *Polym. Chem.* **2016**, *7*, 722; d) P. Murto, A.

Minotto, A. Zampetti, X. Xu, M. R. Andersson, F. Cacialli, E. Wang, *Advanced Optical Materials* **2016**, *4*, 2068.

[36] J. D. Luo, Z. L. Xie, J. W. Y. Lam, L. Cheng, H. Y. Chen, C. F. Qiu, H. S. Kwok, X. W. Zhan, Y. Q. Liu, D. B. Zhu, B. Z. Tang, *Chemical Communications* **2001**, DOI: 10.1039/b105159h1740.

[37] a) Z. J. Zhao, S. M. Chen, J. W. Y. Lam, C. K. W. Jim, C. Y. K. Chan, Z. M. Wang, P. Lu, C. M. Deng, H. S. Kwok, Y. G. Ma, B. Z. Tang, *Journal of Physical Chemistry C* **2010**, *114*, 7963; b) J. Chen, C. C. W. Law, J. W. Y. Lam, Y. Dong, S. M. F. Lo, I. D. Williams, D. Zhu, B. Z. Tang, *Chemistry of Materials* **2003**, *15*, 1535; c) Y. Hong, J. W. Y. Lam, B. Z. Tang, *Chemical Communications* **2009**, DOI: 10.1039/B904665H4332; d) J. W. Y. Lam, J. Chen, C. C. W. Law, H. Peng, Z. Xie, K. K. L. Cheuk, H. S. Kwok, B. Z. Tang, *Macromol. Symp.* **2003**, *196*, 289; e) R. Zhan, Y. Pan, P. N. Manghnani, B. Liu, *Macromolecular bioscience* **2017**, *17*, 1600433.

[38] a) Y. N. Hong, J. W. Y. Lam, B. Z. Tang, *Chemical Communications* **2009**, DOI: 10.1039/b904665h4332; b) A. J. Qin, J. W. Y. Lam, L. Tang, C. K. W. Jim, H. Zhao, J. Z. Sun, B. Z. Tang, *Macromolecules* **2009**, *42*, 1421; c) W. X. Tang, Y. Xiang, A. J. Tong, *Journal of Organic Chemistry* **2009**, *74*, 2163.

[39] a) X. Du, J. Qi, Z. Zhang, D. Ma, Z. Y. Wang, *Chemistry of Materials* **2012**, *24*, 2178; b) S. Wang, X. Yan, Z. Cheng, H. Zhang, Y. Liu, Y. Wang, *Angewandte Chemie International Edition* **2015**, *54*, 13068; c) S. Baysec, A. Minotto, P. Klein, S. Poddi, A. Zampetti, S. Allard, F. Cacialli, U. Scherf, *Science China-Chemistry* **2018**, *61*, 932; d) D. Wang, M. M. S. Lee, G. G. Shan, R. T. K. Kwok, J. W. Y. Lam, H. F. Su, Y. C. Cai, B. Z. Tang, *Advanced Materials* **2018**, *30*, 9.

[40] a) J. V. Caspar, E. M. Kober, B. P. Sullivan, T. J. Meyer, *Journal of the American Chemical Society* **1982**, *104*, 630; b) S. D. Cummings, R. Eisenberg, *Journal of the American Chemical Society* **1996**, *118*, 1949; c) J. S. Wilson, N. Chawdhury, M. R. A. Al-Mandhary, M. Younus, M. S. Khan, P. R. Raithby, A. Köhler, R. H. Friend, *Journal of the American Chemical Society* **2001**, *123*, 9412; d) U. Mayerhöffer, M. Gsänger, M. Stolte, B. Fimmel, F. Würthner, *Chemistry - A European Journal* **2013**, *19*, 218.

[41] G. M. Fischer, C. Jüngst, M. Isomäki-Krondahl, D. Gauss, H. M. Möller, E. Daltrozzo, A. Zumbusch, *Chemical Communications* **2010**, *46*, 5289.

[42] U. Mayerhoffer, M. Gsanger, M. Stolte, B. Fimmel, F. Wurthner, *Chemistry* **2013**, *19*, 218.

[43] C. Adachi, M. A. Baldo, M. E. Thompson, S. R. Forrest, *Journal of Applied Physics* **2001**, *90*, 5048.

[44] J.-S. Kim, P. K. H. Ho, N. C. Greenham, R. H. Friend, *Journal of Applied Physics* **2000**, *88*, 1073.

[45] a) Y. Cao, I. D. Parker, G. Yu, C. Zhang, A. J. Heeger, *Nature* **1999**, *397*, 414; b) S. Höfle, A. Schienle, M. Bruns, U. Lemmer, A. Colsmann, *Advanced Materials* **2014**, *26*, 2750; c) E. Forsythe, M. Abkowitz, Y. Gao, *The Journal of Physical Chemistry B* **2000**, *104*, 3948; d) J.-S. Kim, R. H. Friend, I. Grizzi, J. H. Burroughes, *Applied Physics Letters* **2005**, *87*, 023506.

[46] F. Cacialli, R. H. Friend, N. Haylett, R. Daik, W. J. Feast, D. A. dosSantos, J. L. Bredas, *Applied Physics Letters* **1996**, *69*, 3794.

[47] A. C. Grimsdale, F. Cacialli, J. Gruner, X. C. Li, A. B. Holmes, S. C. Moratti, R. H. Friend, *Synthetic Metals* **1996**, *76*, 165.

[48] M. Segal, M. A. Baldo, R. J. Holmes, S. R. Forrest, Z. G. Soos, *Physical Review B* **2003**, *68*.

[49] A. Dey, A. Rao, D. Kabra, *Advanced Optical Materials* **2017**, *5*.
[50] R. Curry, W. Gillin, *Applied physics letters* **1999**, *75*, 1380.
[51] R. Sun, Y. Wang, Q. Zheng, H. Zhang, A. Epstein, *Journal of Applied Physics* **2000**, *87*, 7589.
[52] L. H. Slooff, A. Polman, F. Cacialli, R. H. Friend, G. A. Hebbink, F. van Veggel, D. N. Reinhoudt, *Applied Physics Letters* **2001**, *78*, 2122.
[53] B. S. Harrison, T. J. Foley, M. Bouguettaya, J. M. Boncella, J. R. Reynolds, K. S. Schanze, J. Shim, P. H. Holloway, G. Padmanaban, S. Ramakrishnan, *Applied Physics Letters* **2001**, *79*, 3770.
[54] T. C. Lee, J. Y. Hung, Y. Chi, Y. M. Cheng, G. H. Lee, P. T. Chou, C. C. Chen, C. H. Chang, C. C. Wu, *Advanced Functional Materials* **2009**, *19*, 2639.
[55] E. L. Williams, J. Li, G. E. Jabbour, *Applied physics letters* **2006**, *89*, 3506.
[56] J. Xue, L. Xin, J. Hou, L. Duan, R. Wang, Y. Wei, J. Qiao, *Chemistry of Materials* **2017**, *29*, 4775.
[57] S. Kesarkar, W. Mróz, M. Penconi, M. Pasini, S. Destri, M. Cazzaniga, D. Ceresoli, P. R. Mussini, C. Baldoli, U. Giovanella, *Angewandte Chemie International Edition* **2016**, *55*, 2714.
[58] L. Xin, J. Xue, G. Lei, J. Qiao, *RSC Advances* **2015**, *5*, 42354.
[59] R. Tao, J. Qiao, G. Zhang, L. Duan, C. Chen, L. Wang, Y. Qiu, *Journal of Materials Chemistry C* **2013**, *1*, 6446.
[60] M. Cocchi, D. Virgili, V. Fattori, J. Williams, J. Kalinowski, *Applied physics letters* **2007**, *90*, 023506.
[61] Y. Sun, C. Borek, K. Hanson, P. I. Djurovich, M. E. Thompson, J. Brooks, J. J. Brown, S. R. Forrest, *Applied physics letters* **2007**, *90*, 3503.
[62] C. Borek, K. Hanson, P. I. Djurovich, M. E. Thompson, K. Aznavour, R. Bau, Y. Sun, S. R. Forrest, J. Brooks, L. Michalski, *Angewandte Chemie* **2007**, *119*, 1127.
[63] L. Huang, C. Park, T. Fleetham, J. Li, *Applied Physics Letters* **2016**, *109*, 233302.
[64] J. R. Sommer, R. T. Farley, K. R. Graham, Y. Yang, J. R. Reynolds, J. Xue, K. S. Schanze, *ACS Applied Materials & Interfaces* **2009**, *1*, 274.
[65] K. R. Graham, Y. Yang, J. R. Sommer, A. H. Shelton, K. S. Schanze, J. Xue, J. R. Reynolds, *Chemistry of Materials* **2011**, *23*, 5305.
[66] H. B. Wei, G. Yu, Z. F. Zhao, Z. W. Liu, Z. Q. Bian, C. H. Huang, *Dalton Transactions* **2013**, *42*, 8951.
[67] J. Kido, W. Ikeda, M. Kimura, K. Nagai, *Japanese Journal of Applied Physics Part 2-Letters* **1996**, *35*, L394.
[68] a) L. Slooff, A. Polman, F. Cacialli, R. Friend, G. Hebbink, F. Van Veggel, D. Reinhoudt, *Applied physics letters* **2001**, *78*, 2122; b) R. J. Curry, W. P. Gillin, A. P. Knights, R. Gwilliam, *Applied Physics Letters* **2000**, *77*, 2271; c) O. M. Khreis, R. J. Curry, M. Somerton, W. P. Gillin, *Journal of Applied Physics* **2000**, *88*, 777.
[69] W. Gillin, R. Curry, *Applied physics letters* **1999**, *74*, 798.
[70] a) Y. Kawamura, Y. Wada, S. Yanagida, *Jpn. J. Appl. Phys., Part 1* **2001**, *40*, 350; b) A. O'Riordan, E. O'Connor, S. Moynihan, P. Nockemann, P. Fias, R. Van Deun, D. Cupertino, P. Mackie, G. Redmond, *Thin Solid Films* **2006**, *497*, 299.
[71] a) M. A. Baldo, S. Lamansky, P. E. Burrows, M. E. Thompson, S. R. Forrest, *Applied Physics Letters* **1999**, *75*, 4; b) V. Cleave, G. Yahioglu, P. Le Barny, R. H. Friend, N. Tessler, *Advanced Materials* **1999**, *11*, 285; c) M. A. Baldo, M. E. Thompson, S. R. Forrest, *Nature* **2000**, *403*, 750; d) C. Adachi, M. A. Baldo, S. R. Forrest, M. E. Thompson, *Applied Physics Letters* **2000**, *77*, 904; e) S. Lamansky, P. Djurovich, D.

Murphy, F. Abdel-Razzaq, H. E. Lee, C. Adachi, P. E. Burrows, S. R. Forrest, M. E. Thompson, *Journal of the American Chemical Society* **2001**, *123*, 4304; f) B. S. Harrison, T. J. Foley, A. S. Knefely, J. K. Mwaura, G. B. Cunningham, T. S. Kang, M. Bouguettaya, J. M. Boncella, J. R. Reynolds, K. S. Schanze, *Chemistry of Materials* **2004**, *16*, 2938.

[72] E. L. Williams, J. Li, G. E. Jabbour, *Applied physics letters* **2006**, *89*, 083506.

[73] T. Tsuzuki, S. Tokito, *Advanced Materials* **2007**, *19*, 276.

[74] a) Y. Sun, C. Borek, K. Hanson, P. I. Djurovich, M. E. Thompson, J. Brooks, J. J. Brown, S. R. Forrest, *Applied physics letters* **2007**, *90*, 213503; b) J. R. Sommer, R. T. Farley, K. R. Graham, Y. Yang, J. R. Reynolds, J. Xue, K. S. Schanze, *ACS applied materials & interfaces* **2009**, *1*, 274; c) C. Borek, K. Hanson, P. I. Djurovich, M. E. Thompson, K. Aznavour, R. Bau, Y. Sun, S. R. Forrest, J. Brooks, L. Michalski, J. Brown, *Angewandte Chemie* **2007**, *119*, 1127.

[75] a) D. O'Brien, C. Giebeler, R. Fletcher, A. Cadby, L. Palilis, D. Lidzey, P. Lane, D. Bradley, W. Blau, *Synthetic Metals* **2001**, *116*, 379; b) T.-F. Guo, S.-C. Chang, Y. Yang, R. C. Kwong, M. E. Thompson, *Organic Electronics* **2000**, *1*, 15; c) R. C. Kwong, S. Sibley, T. Dubovoy, M. Baldo, S. R. Forrest, M. E. Thompson, *Chemistry of Materials* **1999**, *11*, 3709; d) C.-T. Chen, *Chemistry of Materials* **2004**, *16*, 4389.

[76] a) D. F. O'Brien, M. A. Baldo, M. E. Thompson, S. R. Forrest, *Applied Physics Letters* **1999**, *74*, 442; b) M. Ikai, F. Ishikawa, N. Aratani, A. Osuka, S. Kawabata, T. Kajioka, H. Takeuchi, H. Fujikawa, Y. Taga, *Advanced Functional Materials* **2006**, *16*, 515.

[77] K. R. Graham, Y. Yang, J. R. Sommer, A. H. Shelton, K. S. Schanze, J. Xue, J. R. Reynolds, *Chemistry of Materials* **2011**, *23*, 5305.

[78] D. M. E. Freeman, G. Tregnago, S. A. Rodriguez, K. J. Fallon, F. Cacialli, H. Bronstein, *Journal of Organic Semiconductors* **2015**, *3*, 1.

[79] a) J. Morgado, F. Cacialli, R. H. Friend, R. Iqbal, G. Yahioglu, L. R. Milgrom, S. C. Moratti, A. B. Holmes, *Chemical Physics Letters* **2000**, *325*, 552; b) R. Iqbal, S. C. Moratti, A. B. Holmes, G. Yahioglu, L. R. Milgrom, F. Cacialli, J. Morgado, R. H. Friend, *J. Mater. Sci.-Mater. Electron.* **2000**, *11*, 97; c) J. Morgado, F. Cacialli, R. Iqbal, S. C. Moratti, A. B. Holmes, G. Yahioglu, L. R. Milgrom, R. H. Friend, *Journal of Materials Chemistry* **2001**, *11*, 278.

[80] a) S. R. Yost, J. Lee, M. W. B. Wilson, T. Wu, D. P. McMahon, R. R. Parkhurst, N. J. Thompson, D. N. Congreve, A. Rao, K. Johnson, M. Y. Sfeir, M. G. Bawendi, T. M. Swager, R. H. Friend, M. A. Baldo, T. Van Voorhis, *Nature chemistry* **2014**, *6*, 492; b) M. W. B. Wilson, A. Rao, J. Clark, R. S. S. Kumar, D. Brida, G. Cerullo, R. H. Friend, *Journal of the American Chemical Society* **2011**, *133*, 11830; c) B. J. Walker, A. J. Musser, D. Beljonne, R. H. Friend, *Nature chemistry* **2013**, *5*, 1019; d) A. Rao, M. W. B. Wilson, J. M. Hodgkiss, S. Albert-Seifried, H. Bassler, R. H. Friend, *Journal of the American Chemical Society* **2010**, *132*, 12698.

[81] R. Nagata, H. Nakanotani, W. J. Potscavage, C. Adachi, *Advanced Materials* **2018**, *30*.

[82] a) H. Uoyama, K. Goushi, K. Shizu, H. Nomura, C. Adachi, *Nature* **2012**, *492*, 234; b) F. B. Dias, T. J. Penfold, A. P. Monkman, *Methods and Applications in Fluorescence* **2017**, *5*, 012001.

[83] a) S. Hirata, Y. Sakai, K. Masui, H. Tanaka, S. Y. Lee, H. Nomura, N. Nakamura, M. Yasumatsu, H. Nakanotani, Q. Zhang, K. Shizu, H. Miyazaki, C. Adachi, *Nature materials* **2015**, *14*, 330; b) H. Nakanotani, T. Higuchi, T. Furukawa, K. Masui, K. Morimoto, M. Numata, H. Tanaka, Y. Sagara, T. Yasuda, C. Adachi, *Nature*

communications **2014**, *5*, 4016; c) T. Higuchi, H. Nakanotani, C. Adachi, *Advanced Materials* **2015**, *27*, 2019.

[84] a) A. S. Dhoot, N. C. Greenham, *Advanced Materials* **2002**, *14*, 1834; b) D. Y. Kondakov, T. D. Pawlik, T. K. Hatwar, J. P. Spindler, *Journal of Applied Physics* **2009**, *106*, 7; c) B. H. Wallikewitz, D. Kabra, S. Gelinas, R. H. Friend, *Physical Review B* **2012**, *85*, 15; d) C. Mayr, T. D. Schmidt, W. Brutting, *Applied Physics Letters* **2014**, *105*.

[85] a) S. Y. Lee, T. Yasuda, H. Komiyama, J. Lee, C. Adachi, *Advanced Materials* **2016**, *28*, 4019; b) D. M. E. Freeman, A. J. Musser, J. M. Frost, H. L. Stern, A. K. Forster, K. J. Fallon, A. G. Rapidis, F. Cacialli, I. McCulloch, T. M. Clarke, R. H. Friend, H. Bronstein, *Journal of the American Chemical Society* **2017**, *139*, 11073.

[86] a) P. Data, P. Pander, M. Okazaki, Y. Takeda, S. Minakata, A. P. Monkman, *Angewandte Chemie - International Edition* **2016**, *55*, 5739; b) K. Sun, Y. Sun, D. Liu, Y. Feng, X. Zhang, Y. Sun, W. Jiang, *Dyes and Pigments* **2017**, *147*, 436; c) K. Sun, D. Chu, Y. Cui, W. Tian, Y. Sun, W. Jiang, *Organic Electronics: physics, materials, applications* **2017**, *48*, 389; d) C. Li, R. Duan, B. Liang, G. Han, S. Wang, K. Ye, Y. Liu, Y. Yi, Y. Wang, *Angewandte Chemie - International Edition* **2017**, *56*, 11525.

[87] Y. Yuan, Y. Hu, Y. X. Zhang, J. D. Lin, Y. K. Wang, Z. Q. Jiang, L. S. Liao, S. T. Lee, *Advanced Functional Materials* **2017**, *27*, 1700986.

[88] D.-H. Kim, A. D'Aléo, X.-K. Chen, A. D. Sandanayaka, D. Yao, L. Zhao, T. Komino, E. Zaborova, G. Canard, Y. Tsuchiya, *Nature Photonics* **2018**, *12*, 98.

[89] Y. Yuan, Y. Hu, Y.-X. Zhang, J.-D. Lin, Y.-K. Wang, Z.-Q. Jiang, L.-S. Liao, S.-T. Lee, *Advanced Functional Materials* **2017**, *27*, 1700986.

[90] R. Nagata, H. Nakanotani, C. Adachi, *Advanced Materials* **2017**, *29*, 1604265.

[91] Y. Hu, Y. Yuan, Y.-l. Shi, D. Li, Z.-q. Jiang, L.-s. Liao, *Advanced Functional Materials* **2018**, *28*, 1802597.

[92] a) D. Zhang, L. Duan, C. Li, Y. Li, H. Li, D. Zhang, Y. Qiu, *Advanced Materials* **2014**, *26*, 5050; b) J. Xue, Q. Liang, Y. Zhang, R. Zhang, L. Duan, J. Qiao, *Advanced Functional Materials* **2017**, *27*, 1703283.

[93] R. Nagata, H. Nakanotani, C. Adachi, *Advanced Materials* **2017**, *29*, 1604265.

[94] D. Baigent, P. Hamer, R. Friend, S. Moratti, A. Holmes, *Synthetic Metals* **1995**, *71*, 2175.

[95] R. Iqbal, G. Yahioglu, L. Milgrom, S. C. Moratti, A. B. Holmes, F. Cacialli, J. Morgado, R. H. Friend, *Synthetic Metals* **1999**, *102*, 1024.

[96] J. C. Ostrowski, K. Susumu, M. R. Robinson, M. J. Therien, G. C. Bazan, *Advanced Materials* **2003**, *15*, 1296.

[97] J. Morgado, F. Cacialli, R. Friend, R. Iqbal, G. Yahioglu, L. Milgrom, S. Moratti, A. Holmes, *Chemical Physics Letters* **2000**, *325*, 552.

[98] P. Murto, A. Minotto, A. Zampetti, X. Xu, M. R. Andersson, F. Cacialli, E. Wang, *Advanced Optical Materials* **2016**, *4*, 2068.

[99] O. Fenwick, J. K. Sprafke, J. Binas, D. V. Kondratuk, F. Di Stasio, H. L. Anderson, F. Cacialli, *Nano letters* **2011**, *11*, 2451.

[100] S. Ellinger, K. R. Graham, P. Shi, R. T. Farley, T. T. Steckler, R. N. Brookins, P. Taranekar, J. Mei, L. A. Padilha, T. R. Ensley, *Chemistry of Materials* **2011**, *23*, 3805.

[101] B. Stender, S. F. Völker, C. Lambert, J. Pflaum, *Advanced materials* **2013**, *25*, 2943.

[102] M. T. Sharbati, F. Panahi, A. Shourvarzi, S. Khademi, F. Emami, *Optik-International Journal for Light and Electron Optics* **2013**, *124*, 52.

[103] M. X. Chen, E. Perzon, M. R. Andersson, S. Marcinkevicius, S. K. M. Jonsson, M. Fahlman, M. Berggren, *Applied Physics Letters* **2004**, *84*, 3570.
[104] A. Graf, C. Murawski, Y. Zakharko, J. Zaumseil, M. C. Gather, *Advanced Materials* **2018**, *30*, 1706711.
[105] a) A. Zampetti, A. Minotto, F. Cacialli, A. G. Rodriguez, S. Allard, U. Scherf, Ieee, *Low-Gap Polymers Incorporating a Dicarboxylic Imide Moiety for Near-Infrared Polymer Light-Emitting Diodes*, **2015**; b) T. C. Parker, D. G. D. Patel, K. Moudgil, S. Barlow, C. Risko, J.-L. Brédas, J. R. Reynolds, S. R. Marder, *Materials Horizons* **2015**, *2*, 22; c) C. L. Chochos, A. Katsouras, N. Gasparini, C. Koulogiannis, T. Ameri, C. J. Brabec, A. Avgeropoulos, *Macromolecular Rapid Communications* **2017**, *38*.
[106] a) K. Zhang, B. Tieke, *Macromolecules* **2008**, *41*, 7287; b) J. S. Zambounis, Z. Hao, A. Iqbal, *Nature* **1997**, *388*, 131; c) Y. B. Xu, Y. Jin, W. H. Lin, J. B. Peng, H. F. Jiang, D. R. Cao, *Synthetic Metals* **2010**, *160*, 2135; d) S. Stas, J. Y. Balandier, V. Lemaur, O. Fenwick, T. Giulia, F. Quist, F. Cacialli, J. Cornil, Y. H. Geerts, *Dyes and Pigments* **2013**, *97*, 198; e) H. Bronstein, Z. Y. Chen, R. S. Ashraf, W. M. Zhang, J. P. Du, J. R. Durrant, P. S. Tuladhar, K. Song, S. E. Watkins, Y. Geerts, M. M. Wienk, R. A. J. Janssen, T. Anthopoulos, H. Sirringhaus, M. Heeney, I. McCulloch, *Journal of the American Chemical Society* **2011**, *133*, 3272.
[107] T. Beyerlein, B. Tieke, S. Forero-Lenger, W. Brutting, *Synthetic Metals* **2002**, *130*, 115.
[108] P. Li, O. Fenwick, S. Yilmaz, D. Breusov, D. J. Caruana, S. Allard, U. Scherf, F. Cacialli, *Chemical Communications* **2011**, *47*, 8820.
[109] a) G. Winroth, G. Latini, D. Credgington, L.-Y. Wong, L.-L. Chua, P. K.-H. Ho, F. Cacialli, *Applied physics letters* **2008**, *92*, 103308; b) R. Q. Png, P. J. Chia, J. C. Tang, B. Liu, S. Sivaramakrishnan, M. Zhou, S. H. Khong, H. S. O. Chan, J. H. Burroughes, L. L. Chua, R. H. Friend, P. K. H. Ho, *Nature materials* **2010**, *9*, 152.
[110] O. Fenwick, S. Fusco, T. N. Baig, F. Di Stasio, T. T. Steckler, P. Henriksson, C. Flechon, M. R. Andersson, F. Cacialli, *APL Mater.* **2013**, *1*, 7.
[111] F. Lombeck, D. W. Di, L. Yang, L. Meraldi, S. Athanasopoulos, D. Credgington, M. Sommer, R. H. Friend, *Macromolecules* **2016**, *49*, 9382.
[112] P. Ledwon, P. Zassowski, T. Jarosz, M. Lapkowski, P. Wagner, V. Cherpak, P. Stakhira, *Journal of Materials Chemistry C* **2016**, *4*, 2219.
[113] a) L. Beverina, P. Salice, *European Journal of Organic Chemistry* **2010**, DOI: 10.1002/ejoc.2009012971207; b) S. Yagi, H. Nakazumi, in *Heterocyclic Polymethine Dyes: Synthesis, Properties and Applications*, Vol. 14 (Ed: L. Strekowski) **2008**, p. 133; c) A. Ajayaghosh, *Chemical Society Reviews* **2003**, *32*, 181; d) A. Ajayaghosh, *Accounts of chemical research* **2005**, *38*, 449; e) S. Sreejith, P. Carol, P. Chithra, A. Ajayaghosh, *Journal of Materials Chemistry* **2008**, *18*, 264; f) S. Sreejith, K. P. Divya, A. Ajayaghosh, *Angewandte Chemie-International Edition* **2008**, *47*, 7883.
[114] a) J. H. Yum, P. Walter, S. Huber, D. Rentsch, T. Geiger, F. Nuesch, F. De Angelis, M. Gratzel, M. K. Nazeeruddin, *Journal of the American Chemical Society* **2007**, *129*, 10320; b) G. D. Wei, S. Y. Wang, K. Sun, M. E. Thompson, S. R. Forrest, *Advanced Energy Materials* **2011**, *1*, 184; c) F. Silvestri, M. D. Irwin, L. Beverina, A. Facchetti, G. A. Pagani, T. J. Marks, *Journal of the American Chemical Society* **2008**, *130*, 17640.
[115] H. H. Nho, H. Bae, W. Yao, Y. Li, A. Al-Dahle, Google Patents, 2017.
[116] K. Ghaffarzadeh, N. Bardsley, *OLED Lighting Opportunities 2017-2027: Forecasts, Technologies, Players*, **2017**.
[117] a) S. Yoo, S. Hong, Y. Choi, J. H. Park, Y. Nam, *ACS nano* **2014**, *8*, 8040; b) M. H. Ryu, I. H. Kang, M. D. Nelson, T. M. Jensen, A. I. Lyuksyutova, J. Siltberg-Liberles,

D. M. Raizen, M. Gomelsky, *Proceedings of the National Academy of Sciences of the United States of America* **2014**, *111*, 10167; c) Y. Lyu, C. Xie, S. A. Chechetka, E. Miyako, K. Y. Pu, *Journal of the American Chemical Society* **2016**, *138*, 9049; d) K. Huang, Q. Q. Dou, X. J. Loh, *Rsc Advances* **2016**, *6*, 60896.

[118] P. K. Jain, V. Ramanan, A. G. Schepers, N. S. Dalvie, A. Panda, H. E. Fleming, S. N. Bhatia, *Angewandte Chemie-International Edition* **2016**, *55*, 12440.

[119] L. P. Toth, C. A. Gersbach, *Molecular Therapy* **2015**, *23*, S275.

[120] a) G. J. Supran, K. W. Song, G. W. Hwang, R. E. Correa, J. Scherer, E. A. Dauler, Y. Shirasaki, M. G. Bawendi, V. Bulovic, *Advanced Materials* **2015**, *27*, 1437; b) J. S. Steckel, S. Coe-Sullivan, V. Bulovic, M. G. Bawendi, *Advanced Materials* **2003**, *15*, 1862.

[121] a) R. Capelli, S. Toffanin, G. Generali, H. Usta, A. Facchetti, M. Muccini, *Nature materials* **2010**, *9*, 496; b) R. Capelli, J. J. Amsden, G. Generali, S. Toffanin, V. Benfenati, M. Muccini, D. L. Kaplan, F. G. Omenetto, R. Zamboni, *Organic Electronics* **2011**, *12*, 1146.

[122] A. Graf, M. Held, Y. Zakharko, L. Tropf, M. C. Gather, J. Zaumseil, *Nature materials* **2017**, *16*, 911.

[123] a) G. M. Fischer, A. R. Ehlers, A. Zumbusch, E. Daltrozzo, *Angewandte Chemie-International Edition* **2007**, *46*, 3750; b) A. Leventis, J. Royakkers, A. G. Rapidis, N. Goodeal, M. K. Corpinot, J. M. Frost, D. K. Bucar, M. O. Blunt, F. Cacialli, H. Bronstein, *Journal of the American Chemical Society* **2018**, *140*, 1622.

[124] a) R. K. Pal, S. C. Kundu, V. K. Yadavalli, *Acs Applied Materials & Interfaces* **2018**, *10*, 9620; b) L. Migliaccio, S. Aprano, L. Iannuzzi, M. G. Maglione, P. Tassini, C. Minarini, P. Manini, A. Pezzella, *Advanced Electronic Materials* **2017**, *3*; c) M. Berggren, A. Richter-Dahlfors, *Advanced Materials* **2007**, *19*, 3201.

[125] a) Q. M. Peng, A. Obolda, M. Zhang, F. Li, *Angewandte Chemie-International Edition* **2015**, *54*, 7091; b) A. Obolda, M. Zhang, F. Li, *Chinese Chemical Letters* **2016**, *27*, 1345; c) A. Obolda, X. Ai, M. Zhang, F. Li, *Acs Applied Materials & Interfaces* **2016**, *8*, 35472.